C.P. No. 830

C.P. No. 830

MINISTRY OF AVIATION

AERONAUTICAL RESEARCH COUNCIL

CURRENT PAPERS

Slender-Body Theory Calculations of the Effect on Lift and Moment of Mounting the Wing off the Fuselage Centre-Line

by

R. S. Bartlett, M.A.

LONDON: HER MAJESTY'S STATIONERY OFFICE

1965

PRICE 11*s* 6*d* NET

U.D.C. No. 533.695.12 : 533.6.013.13 : 533.6.013.15

C.P. No.830

February 1964

SLENDER-BODY THEORY CALCULATIONS OF THE EFFECT ON LIFT AND MOMENT OF MOUNTING THE WING OFF THE FUSELAGE CENTRE-LINE

by

R. S. Bartlett, M.A.

SUMMARY

Slender-body theory is used to calculate the effects on lift and moment of mounting the wing of a wing-body combination above or below the body axis, with and without wing-body angle. The wing must have a local span which increases in the downstream direction, an unswept trailing edge and uncambered cross-sections. The cross-sections of the body are assumed to be circles of constant radius over the length of the wing.

It is found that the effects of the asymmetrical mounting are substantial when the body diameter is more than half the wing span, but fall off as the body shrinks. For a typical aircraft configuration, the pitching moment is found to be more affected than the lift.

Replaces R.A.E. Tech. Note No. Aero 2950 - A.R.C. 25 965.

CONTENTS

APPENDICES

TABLES

ILLUSTRATIONS

1 INTRODUCTION

A possible shape for a supersonic aircraft or missile is basically a wing of nearly triangular planform shape mounted on a body of almost circular cross-section. In the case of the aircraft, the wing may well not be mounted symmetrically on the body for non-aerodynamic reasons. The present paper is intended to help in the assessment of the effects on lift and, more significantly, on pitching moment of asymmetric wing mounting, with and without wing-body angle.

The configuration studied comprises a wing with a swept-back leading edge, a local span increasing in the stream direction and an unswept trailing edge, which is mounted on a body, possibly cambered, whose cross-sections are circles of constant diameter over the length of the wing. The wing may be curved in the streamwise direction only; it may be set on the body at a wing-body angle which varies along its length and any asymmetry in the mounting of the wing on the body is taken into account in the theory.

The flow is assumed not to separate from the configuration ahead of the wing trailing edge and the effects of viscosity are supposed to be confined to thin boundary layers on the surface and to the wake. Disturbances are assumed to be small, thus allowing the use of the linearized approximation to the equations of inviscid compressible flow, and the further assumption is made that the velocities change slowly in the streamwise direction relative to their rates of change across the stream. Slender-body theory is then applicable and the effects of cross-sectional shape can be brought in through the use of conformal transformation. The appropriate transformations have been used previously by Pepper[1] in a Trefftz-plane study of minimum induced drag configurations at low speeds.

The theory expresses the lift acting on that part of the configuration ahead of a plane normal to the main stream (a 'cross flow' plane) in terms of the shape and streamwise slope of the section of the configuration by this plane. The pitching moment is readily obtained from the general results for the lift by a single integration. Results have previously been given by Dugan and Hikido[2] and by Stocker[3] for the case of the symmetrically mounted wing with and without wing-body angle, though the latter has a wrong sign in his formula. For the asymmetrical configuration at a common incidence we now obtain an expression for the lift in closed form. When the wing and body incidences differ, we are unable to evaluate the integral expression for the lift in terms of familiar functions and resort to numerical integration. The lift is, of course, linear in the wing-body angle, but the coefficient depends on two independent variables, a span to radius ratio and a parameter measuring the asymmetry. The dependence of the coefficient on these variables is displayed graphically and in a table.

Unless the free-stream Mach number is close to one, when other effects make the application of linearized theories like the present one doubtful, the calculation of lifting effects by slender-body theory is adequate only for very slender shapes. Very slender wings have highly swept leading edges with the component of the free-stream velocity normal to them well subsonic. Under these conditions the flow normally separates from the leading edges, and vortices are formed above and inboard of them. The omission of any representation of these from the present theory makes the direct application of it to very slender wings also unreliable, except at an incidence for which the flow is attached. Thus for a plane wing or symmetrical wing-body combination, we should expect the theory to provide the lift slope and aerodynamic centre at zero incidence if the wing is very slender. If the wing is warped so that at some incidence there are attachment lines along the leading edges, the attached flow theory will be adequate for the lift, centre of pressure, lift slope and aerodynamic centre at this incidence. Such warp generally includes camber of the wing cross-sections and the present treatment makes no attempt to represent this. It could be represented to the accuracy of slender thin-wing theory (which involves the usual assumption of thin-wing theory that surface boundary conditions can be applied on a mean plane) by use of the same conformal transformations as are used here, but a treatment by slender-body theory would be much more complicated. Hence, except in the trivial case of the symmetrical configurations, or the very special case in which the singularities in the load at the wing leading edge produced by wing incidence and by body incidence of the opposite sign just cancel, the present model of the flow is not adequate.

On the other hand, in circumstances in which we are prepared to accept that small corrections are additive, the present results can be used to estimate the corrections due to wing-body asymmetry. Such an assumption has already been made by Pitts, Nielsen and Kaattari[4] in an attempt to account for the effects of a symmetrically mounted body on the lift and moment of a wing. They use slender-body theory for the symmetrical wing-body combination in conjunction with supersonic thin-wing theory for the wing alone to obtain results for wing-body combinations to which the unmodified slender-body theory could not fruitfully be applied. Since they obtain satisfactory agreement with experiment, we may expect the present results to be usable in the same way. Apart then from the intrinsic interest of the present results, and their value in indicating the orders of the effects involved, their utility is expected to lie in providing data for the evaluation of the effects of wing asymmetry along the lines of Ref.4. Since even in the symmetrical case, for which quasi-cylinder theory has been formulated, resort to slender-body theory has been found necessary in practice, we may suppose that any more elaborate approach to the effects of asymmetry would be impracticable.

As an example, a configuration somewhat resembling a supersonic transport aircraft is treated by the present method and the shifts in the centre of pressure and aerodynamic centre positions from the wing alone values owing to the addition of the body are found, both including and disregarding the asymmetry of the mounting. The effects of asymmetry are found to be small, but significant for a slender aircraft.

2 FORMULATION OF THE PROBLEM

We consider a configuration consisting of a wing without thickness mounted on a fuselage in a supersonic stream. The wing planform has a straight unswept trailing edge, its leading edge is swept back so that the component of the free stream normal to it is subsonic and the local span increases monotonically in the streamwise direction. The wing is allowed to have lengthwise camber, that is, its surface slope is a function of the streamwise co-ordinate only. The fuselage is slender and smooth, with a pointed apex somewhere upstream of the wing root and circular cross-sections over the length of the wing. The fuselage is also allowed to have lengthwise camber, which may be different from that of the wing.

We introduce right-handed rectangular axes with origin O at the fuselage nose, Ox in the stream direction and Oy to starboard.

The local incidences of the wing and fuselage are assumed to be small so that the disturbances of the uniform stream are also small. Then a disturbance velocity potential, ϕ, exists and satisfies the equation

$$(1 - M^2)\,\phi_{xx} + \phi_{yy} + \phi_{zz} = 0 \quad . \tag{1}$$

Under the additional assumption of the slender body theory of Munk, Jones and Ward[5], that the streamwise rates of change of velocity are small compared to variations in the cross-flow plane, equation (1) reduces to Laplace's equation in planes normal to the stream:

$$\phi_{yy} + \phi_{zz} = 0 \quad . \tag{2}$$

The disturbance potential near the body can be expressed as the mean of two terms

$$\phi(x,y,z) = \phi_1(y,z;x) + \phi_2(x)$$

of which the second vanishes identically for those values of x for which the cross-sectional area of the configuration is constant. In the present case we are not concerned with the properties of the nose of the configuration ahead of the wing root or of any afterbody behind the wing trailing edge, and ϕ_2 is zero for the length of the wing. The disturbance potential then tends to zero as the distance from the body increases laterally and, in combination with the undisturbed stream, satisfies the usual condition of no flow through the surface of the configuration. This condition can be expressed as

$$(U + \phi_x)\,F_x + \phi_y\,F_y + \phi_z\,F_z = 0 \tag{3}$$

where $F(x,y,z) = 0$ is the equation of the surface of the configuration.

Suppose the equation of the wing and fuselage surfaces are respectively

$$z + g(x) = 0, \quad \text{for } -S(x) \leqslant y \leqslant -\bar{R}(x) \quad \text{and} \quad \bar{R}(x) \leqslant y \leqslant S(x)$$

and

$$y^2 + [z + h(x)]^2 - R^2 = 0$$

where $g(x)$ and $h(x)$ are the distances of the wing and the centre line of the fuselage below the x axis, $S(x)$ is the semispan of the wing and $y = \pm\bar{R}(x)$, $z = -g(x)$ defines the wing fuselage function (see Fig.1A).

It is consistent with the assumption of small disturbances to neglect ϕ_x in comparison with U, so that the boundary conditions on the surface become

$$\left.\begin{array}{ll} \text{on the wing:} & U\, g'(x) + \phi_z = 0 \\ \text{on the fuselage:} & U(z+h)\, h'(x) + y\, \phi_y + (z+h)\, \phi_z = 0 \ . \end{array}\right\} \quad (4)$$

Now, in the notation of Fig.1B,

$$\phi_y \cos\theta - \phi_z \sin\theta = \phi_n$$

that is

$$y\, \phi_y + (z+h)\, \phi_z = R\, \phi_n \quad (5)$$

where n is the outward normal to the fuselage cross-section, so the boundary conditions prescribe the normal derivative of ϕ on the cross-section of the configuration (Fig.1A).

Since ϕ is a solution of equation (2) it is the real part of an analytic function $W(\chi)$, where $\chi = y + i\, z$. If χ' is an analytic function of χ, then W is also an analytic function of χ', so we can apply a conformal transformation to the χ plane to obtain a simpler boundary in the χ' plane. The normal velocities at corresponding points of the boundaries will then be related by

$$\frac{\phi_n'}{\phi_n} = \left|\frac{d\chi}{d\chi'}\right| \ . \quad (6)$$

It is convenient to simplify the fuselage boundary condition by the superposition of a uniform cross flow parallel to the imaginary axis in the χ plane. We introduce

$$\phi^* = \phi + U\, z\, h'(x) \quad (7)$$

so that the equations (4) become

$$\begin{array}{ll} \text{on the wing:} & U[g'(x) - h'(x)] + \phi_z^* = 0 \\ \text{on the fuselage:} & y\, \phi_y^* + (z+h)\, \phi_z^* = 0 \end{array}$$

or, in virtue of equation (5),

$$\left.\begin{aligned} \phi_n^* &= 0 \text{ on the fuselage} \\ &\text{and} \\ \phi_n^* &= \mp U[\alpha_W(x) - \alpha_B(x)] \text{ on the upper and lower surfaces of the wing} \end{aligned}\right\} \quad (8)$$

where $\alpha_W = g'$ is the wing incidence and $\alpha_B = h'$ is the fuselage incidence. We now seek a complex function W^* whose real part ϕ^* satisfies the equations (8) and behaves like $U\,\alpha_B\,Z$ at large distances.

It will be seen to be sufficient to limit the investigation to positive values of $(h - g)$, since the expression for lift is an (implicit) even function in $(h - g)$ owing to the symmetry of the configuration and the linear dependence of the lift on the wing and body incidences.

3 CONSTRUCTION OF THE COMPLEX POTENTIAL

In order to transform the contour of Fig.1A into a simpler form we first observe that $\chi + i\,g$ is real on the wing surfaces HAB and DEF and that the argument of $\dfrac{\chi + i\,g + \bar{R}}{\chi + i\,g - \bar{R}}$ is constant on the fuselage surfaces BCD and FGH. Thus if

$$\zeta = \log \frac{\chi + i\,g + \bar{R}}{\chi + i\,g - \bar{R}} \qquad (9)$$

the imaginary part of ζ takes a constant value on the parts of the contour corresponding to the fuselage and zero on the parts corresponding to the wing. The whole χ-plane is mapped onto the strip of the ζ-plane given by:

$$-\pi \leqslant \mathrm{Im}(\zeta) \leqslant +\pi \quad .$$

The resulting configuration is shown in Fig.2. For large values of χ, $\zeta = \dfrac{2\bar{R}}{\chi} + O(\chi^{-2})$ so the point at infinity in the χ-plane becomes the origin of the ζ-plane and the uniform flow at infinity in the χ-plane becomes a doublet at the origin of the ζ-plane with its axis along the imaginary axis.

Since the contour in the ζ-plane is polygonal, we can transform it into the real axis (of a t-plane) by a Schwartz-Christoffel transformation. We can choose 3 points arbitrarily and it is convenient to let the co-ordinates of the points C and D be 0 and 1, and to make G be the point at infinity in the t-plane, as shown in Fig.3. Then if E and F become d and n, by symmetry H, A and B will become $-n$, $-d$ and -1. The exterior angles of the polygon at A, B, D, E, F and H are $-\pi$, $+\pi$, $+\pi$, $-\pi$, $+\pi$ and $+\pi$ respectively, where we describe the polygon with the wall on the right. Hence

$$\zeta = A\int_0^t \frac{(\lambda + d)\,(\lambda - d)\,d\lambda}{(\lambda + 1)\,(\lambda - 1)\,(\lambda + n)\,(\lambda - n)} + B \quad .$$

Effecting the integration and expressing A and B in terms of n and d we find that

$$\zeta = \beta \log\left(\frac{n + t}{n - t}\right) + (1 - \beta) \log\left(\frac{t + 1}{t - 1}\right) \qquad (10)$$

where

$$d^2 = n\{n(1 - \beta) + \beta\}\,\{n\,\beta + 1 - \beta\}^{-1} \qquad (11)$$

and

$$\log\left(\frac{S + \bar{R}}{S - \bar{R}}\right) = \beta \log\left(\frac{n + d}{n - d}\right) + (1 - \beta) \log\left(\frac{d + 1}{d - 1}\right) \quad . \qquad (12)$$

Equations (9) and (10) determine the transformation of the exterior of the contour in the χ-plane onto the upper half of a t-plane, with indicated corresponding points and the transformation parameters n and d can be determined from equations (11) and (12). This transformation was used by Pepper[1]. The point at infinity in the χ-plane is mapped into the point $\zeta = 0$, and finally into the point $t = i\,S_1$ where

$$0 = \beta \log\left(\frac{n + i\,S_1}{n - i\,S_1}\right) + (1 - \beta) \log\left(\frac{i\,S_1 + 1}{i\,S_1 - 1}\right) \qquad (13A)$$

or, in real terms,

$$\beta \tan^{-1}\left(\frac{S_1}{n}\right) = (1 - \beta) \cot^{-1} S_1 \quad . \qquad (13B)$$

For large values of χ we have

$$t = i\,S_1 + \frac{a_1\,\bar{R}}{\chi} + \frac{a_2\,\bar{R}^2}{\chi^2} + \frac{a_3\,\bar{R}^3}{\chi^3} + O(\chi^{-4}) \qquad (14)$$

where the coefficients a_1, a_2 and a_3 are evaluated in Appendix 2. For large χ the complex potential behaves like

$$-i\,U\,\alpha_B\,\chi = -\frac{i\,U\,\alpha_B\,a_1\,\bar{R}}{(t - i\,S_1)} + O((t - i\,S_1)^{-2})$$

and so the flow at infinity in the χ-plane is represented by a doublet at $t = i\,S_1$ with its axis along the imaginary axis.

The normal velocity on the whole contour can now be made to vanish by the introduction of another doublet, oppositely oriented, at $t = -i\,S_1$. Thus the complex potential

$$i\,U\,\alpha_B\,a_1\,\bar{R}\left(-\frac{1}{t - i\,S_1} + \frac{1}{t + i\,S_1}\right) = \frac{2U\,\alpha_B\,a_1\,S_1\,\bar{R}}{t^2 + S_1^2} \qquad (15)$$

satisfies the boundary condition imposed on W* at infinity and on the fuselage. The boundary condition on the wing can be satisfied by a distribution of sources and sinks along the appropriate parts of the real axis in the t-plane without upsetting the conditions on the fuselage and at infinity. By equations (6) and (8) we require normal velocities in the t-plane of magnitude

$$U(\alpha_W - \alpha_B)\left|\frac{d\chi}{dt}\right| \text{ on HA and EF}$$

and

$$-U(\alpha_W - \alpha_B)\left|\frac{d\chi}{dt}\right| \text{ on AB and DE} \quad .$$

These are produced by source strengths per unit length of twice these values, making a contribution to the complex potential of

$$\frac{U(\alpha_W - \alpha_B)}{\pi}\left\{+\int_H^A - \int_A^B - \int_D^E + \int_E^F \left[|f(\lambda)|\,\log(t - \lambda)\,d\lambda\right]\right\}$$

where $f(t)$ has been written for $\frac{d\chi}{dt}$.

By equations (9), (10) and (11)

$$f(t) = \frac{2(n\,\beta + 1 - \beta)\,(t^2 - d^2)}{(n^2 - t^2)\,(t^2 - 1)} \cdot \frac{R^2 - (\chi(t) + g)^2}{2\bar{R}} \quad . \ (17)$$

For points on the wing this is real; it is negative on HA and EF and positive on AB and DE; and it is an even function of t. Hence, by simplifying equation (16) and combining it with equation (15) we obtain

$$W^* = \frac{2U\,\alpha_B\,a_1\,S_1\,\bar{R}}{t^2 + S_1^2} - \frac{U(\alpha_W - \alpha_B)}{\pi}\int_1^n f(\lambda)\,\log(t^2 - \lambda^2)\,d\lambda \qquad \text{....(18)}$$

and, by equation (7),

$$W = W^* + i\,U\,\alpha_B\,\chi\ . \qquad (19)$$

4 LIFT AND MOMENT ON THE CONFIGURATION

The lift force, L, acting on that part of a slender-body forward of a given cross-flow plane is given by the result of Ward, rederived in Appendix 1:

$$F = i\,L(x) = \rho\,U^2\left[2\pi\,b_1 + \frac{d}{dx}\,\{\chi_g(x)\;S(x)\}\right]$$

where b_1 is the coefficient of $\frac{1}{\chi}$ in the expansion of $\frac{W}{U}$ for large χ; χ_g is the complex coordinate of the centre of area of the cross-section of the body and S is its area. In the present application, $S = \pi\,R^2$ and $\chi_g = -i\,h(x)$ with the result that

$$L(x) = -\pi\,\rho\,U^2(2i\,b_1 + R^2\,\alpha_B)\ . \qquad (20)$$

Combining the results of equations (18) and (19), we have

$$\frac{W}{U} = -i\,\alpha_B\,\chi + \frac{2\alpha_B\,a_1\,S_1\,\bar{R}}{t^2 + S_1^2} - \frac{(\alpha_W - \alpha_B)}{\pi}\int_1^n f(\lambda)\,\log(t^2 - \lambda^2)\,d\lambda\ . \qquad \text{....(21)}$$

The first term makes no contribution to b_1. Using equation (14) we find that the second term contributes

$$i\,\alpha_B\,\bar{R}^2\left(\frac{a_3}{a_1} - \frac{a_2^2}{a_1^2} + \frac{a_1^2}{4S_1^2}\right)\ .$$

$$d = \frac{\mu_o}{\beta} + O(1)$$

$$S_1 = \frac{\nu_o}{\beta} + O(1)$$

where $\lambda_o = \nu_o \cot \frac{1}{\nu_o}$, $\mu_o = \lambda_o(1 + \lambda_o)^{-\frac{1}{2}}$ and $2\pi \frac{R}{S} = \log\left(\frac{\lambda_o + \mu_o}{\lambda_o - \mu_o}\right) + \frac{2}{\mu_o}$. The last of these can be written in terms of ν_o as

$$2\pi \frac{R}{S} = \log\left\{\frac{\sqrt{1 + \nu_o \cot \frac{1}{\nu_o}} + 1}{\sqrt{1 + \nu_o \cot \frac{1}{\nu_o}} - 1}\right\} + \frac{2\sqrt{1 + \nu_o \cot \frac{1}{\nu_o}}}{\nu_o \cot \frac{1}{\nu_o}} .$$

The expressions for a_1', a_2' and a_3', given in Appendix 2, become

$$a_1' = \left(\frac{\lambda_o}{\lambda_o^2 + \nu_o^2} + \frac{1}{\nu_o^2}\right)^{-1} \beta^{-2} + O(\beta^{-1})$$

$$a_2' = -i\,\nu_o\left[\frac{\lambda_o}{(\lambda_o^2 + \nu_o^2)^2} + \frac{1}{\nu_o^4}\right]\left[\frac{\lambda_o}{\lambda_o^2 + \nu_o^2} + \frac{1}{\nu_o^2}\right]^{-3} \beta^{-3} + O(\beta^{-2})$$

and

$$a_3' = -2\nu_o^2\left[\frac{\lambda_o}{(\lambda_o^2 + \nu_o^2)^2} + \frac{1}{\nu_o^4}\right]\left[\frac{\lambda_o}{\lambda_o^2 + \nu_o^2} + \frac{1}{\nu_o^2}\right]^{-5} \beta^{-4}$$

$$- \frac{1}{3}\left[\frac{\lambda_o^3 - 3\lambda_o\nu_o^2}{(\lambda_o^2 + \nu_o^2)^3} - \frac{3}{\nu_o^4}\right]\left[\frac{\lambda_o}{\lambda_o^2 + \nu_o^2} + \frac{1}{\nu_o^2}\right]^{-4} \beta^{-4} + O(\beta^{-3}) .$$

The expression for lift, equation (25), becomes in the limit as $\beta \to 0$

The integral $I\left(\beta, \frac{R}{S}\right)$, equation (22), cannot, apparently, be expressed in terms of familiar functions for general values of β. For $\beta = \frac{1}{2}$, the mounting is symmetrical and the result of Dugan and Hikido can be recovered, as in Appendix 3. When β is zero or unity the integral is no longer defined. Attempts were made to find the form of the integral in the limit $\beta \to 0$, but these were unsuccessful. It was decided that it would be more convenient to evaluate the corresponding integral which arises from an independent transformation of the limiting configuration, as described in Appendix 4, and to check its value against that extrapolated from values for non-zero values of β. For this purpose, and for the convenient presentation of the results, we define the function $J\left(\beta, \frac{R}{S}\right)$:

$$J\left(\beta, \frac{R}{S}\right) = \frac{L\left(x;\ 0,\ \alpha_W - \alpha_B,\ \beta,\ \frac{R}{S}\right)}{\frac{1}{2}\rho\ U^2\ S^2(x)\ (\alpha_W - \alpha_B)}$$

$$= 16\left(\frac{R}{S}\right)^2 a_1(n\,\beta + 1 - \beta)\ I\left(\beta, \frac{R}{S}\right) \quad . \qquad (24)$$

For a typical value of $\frac{R}{S}$, three values of $J\left(\beta, \frac{R}{S}\right)$ are given in the table below:

β	$J\left(\beta, \frac{1}{6}\right)$
0.4 0.2 0.1	5.00414 5.46813 5.82769
0	6.22982 6.22917

The assumption that the function $J\left(\beta, \frac{1}{6}\right)$ satisfies a second order polynomial in $\sin \beta\pi$, exact for $\beta = 0.1$, 0.2 and 0.4, leads to the first value for $J\left(0, \frac{1}{6}\right)$ given above. This is very close to the other value given, differing by only 0.01%. The second value is that calculated directly from the independent transformation mentioned above.

For the case of zero wing-body angle, the independently derived result for $\beta = 0$ agrees with the limit of the expression in equation (22) as $\beta \to 0$ and $\alpha_W = \alpha_B$, as is shown in Appendix 4.

For values of β other than 0 and 1, $I\left(\beta, \frac{R}{S}\right)$ can be evaluated numerically. The range of integration is divided into the two intervals [1,d] and [d,n]. The single singularity in each interval is then removed by the transformations

$$\lambda = 1 + \mu^{\frac{1}{1-\beta}} \quad \text{and} \quad \lambda = n - \mu^{\frac{1}{\beta}}$$

respectively and the integrations are carried out using a Gaussian process on the Mercury computer. In the notation introduced above, we may write

$$\frac{L(x)}{\frac{1}{2}\rho\, U^2\, S^2} = 4\pi\, \alpha_B \left(\frac{R}{S}\right)^2 \left(\frac{a_3}{a_1} - \frac{a_2^2}{a_1^2} + \frac{a_1^2}{4S_1^2}\right) - 2\pi\, \alpha_B \left(\frac{R}{S}\right)^2 + (\alpha_W - \alpha_B)\, J\left(\beta, \frac{R}{S}\right) \quad \ldots.(25)$$

where the value of $\left(\frac{a_3}{a_1} - \frac{a_2^2}{a_1^2} + \frac{a_1^2}{4S_1^2}\right)$ has been evaluated in Appendix 2 as

$$\left(\frac{a_3}{a_1} - \frac{a_2^2}{a_1^2} + \frac{a_1^2}{4S_1^2}\right) = \left\{\frac{1}{3} - a_1^4\, S_1^2 \left[\frac{n\,\beta}{(n^2 + S_1^2)^2} + \frac{1-\beta}{(1 + S_1^2)^2}\right]^2 + \frac{a_1^2}{4S_1^2} - \frac{a_1^3}{3}\left[\frac{n\,\beta(n^2 - 3S_1^2)}{(n^2 + S_1^2)^3} + \frac{(1-\beta)\,(1 - 3S_1^2)}{(1 + S_1^2)^3}\right]\right\} \quad \ldots.(26)$$

where

$$a_1 = \left(\frac{n\,\beta}{n^2 + S_1^2} + \frac{1-\beta}{1 + S_1^2}\right)^{-1} .$$

The pitching moment $M(\bar{x})$, about an axis parallel to Oy and through $x = \bar{x}$, due to the lift force on the configuration between the stations $x = a$ and $x = b$ is given by

$$M(\bar{x}) = -\int_a^b (x - \bar{x}) \frac{dL}{dx} \, dx$$

$$= aL(a) - bL(b) + \bar{x}(L(b) - L(a)) + \int_a^b L(x) \, dx \quad . \qquad (27)$$

5 RESULTS

5.1 General results for the lift

Since the part of the present work which is new is that which uses slender-body theory to take into account the displacement of the wing from the centre-line of the fuselage, it is appropriate to look first at the predictions of slender theory for the case where the displacement is zero. Let us write the lift, L, in the form

$$\frac{L\left(\alpha_B, \alpha_W - \alpha_B, \beta, \frac{R}{S}\right)}{\frac{1}{2}\rho\, U^2\, S^2} = G\left(\beta, \frac{R}{S}\right) \alpha_B + J\left(\beta, \frac{R}{S}\right) (\alpha_W - \alpha_B) \qquad (28)$$

following the form of equation (25). Then $G\left(\frac{1}{2}, \frac{R}{S}\right)$ and $J\left(\frac{1}{2}, \frac{R}{S}\right)$ are the previously known functions expressing the dependence of the lift on the body incidence and the wing-body angle when the wing is mounted symmetrically on the body. They are tabulated in Table 1 and shown in Fig.7 for $0 < R < S$, the range over which they are physically meaningful. As $\frac{R}{S}$ tends to zero, they both tend to 2π, the value for the wing alone; but, as $R \to S$ and the body covers the entire wing, J tends to zero and G tends again to 2π, which is also the value for the body alone. The minimum value of $G\left(\frac{1}{2}, \frac{R}{S}\right)$ occurs for $\frac{R}{S} = 2^{-\frac{1}{2}}$ and is 75% of the maximum.

Since $G\left(\frac{1}{2}, \frac{R}{S}\right)$ is always non-zero, it is convenient to refer $G\left(\beta, \frac{R}{S}\right)$ to it in order to display the effects of β. Now $G\left(\beta, \frac{R}{S}\right)$ is defined for $S \geq \bar{R} = R \sin \beta\pi$, as is clear from Fig.1, so it is convenient to extend the range of $G\left(\frac{1}{2}, \frac{R}{S}\right)$ by defining it to be 2π for $R > S$. The function $\tilde{G}\left(\beta, \frac{R}{S}\right)$, where

$$\tilde{G}\left(\beta, \frac{R}{S}\right) = G\left(\beta, \frac{R}{S}\right) \Big/ G\left(\frac{1}{2}, \frac{R}{S}\right) \qquad (29)$$

then defines the change in the lift due to common incidence, α_B, of wing and body caused by a departure from the symmetrical mounting. It can be expressed in closed form from equations (25) and (26) in terms of the geometrical quantities determined by equations (11), (12) and (13). It is tabulated for several values of β as a function of $\frac{R}{S}$ in Table 2(a) and as a function of $\frac{\bar{R}}{S}$ in Table 2(b). It is plotted against $\frac{R}{S}$ and $\frac{S}{R}$ for each of these ratios between 0 and 1 in the left and right halves of Fig.8. The curve for each value of β terminates on the right with $\tilde{G} = 1$ where $S = \bar{R} = R \sin \beta\pi$, corresponding to the vanishing of the wing into the body. The effect of the asymmetry must obviously tend to zero as the exposed wing disappears. Again, each curve terminates on the left with $\tilde{G} = 1$ where $R = 0$ and the effect of asymmetry is once more zero. As would be expected, the value of $\tilde{G}$ for any given value of $\frac{R}{S}$ increases as β departs from 0.5. The maximum value of $\tilde{G}$ for each value of β is attained at some value of $\frac{R}{S}$ between 0.80 and 0.86. The largest of these maxima, for $\beta = 0$, is $\tilde{G}(0, 0.8558) = 1.3445$. Since $\tilde{G}$ is always at least one and $G\left(\frac{1}{2}, \frac{R}{S}\right)$ is never more than 2π, the effects which the presence of the body and the asymmetrical mounting produce on the lift due to common incidence are in opposite senses and the maximum effects never reinforce one another. However, with $R = S$, $G\left(\frac{1}{2}, \frac{R}{S}\right)$ is 2π and an increment of over 25% in lift is indicated by Fig.8 in the extreme case $\beta = 0$, compared with the maximum decrement from 2π of 25% remarked on earlier in the case $\frac{R}{S} = 2^{-\frac{1}{2}}$, $\beta = \frac{1}{2}$. For some purposes it may be more convenient to consider the dependence of $\tilde{G}\left(\beta, \frac{R}{S}\right)$ on $\frac{\bar{R}}{S}$, the proportion of the span actually covered by the body, as in Table 2(b). It is unity for $\frac{\bar{R}}{S} = 0$ provided $\beta \neq 0$ and also for $\frac{\bar{R}}{S} = 1$. It is also unity for $\beta = \frac{1}{2}$ and it tends to unity as $\beta \to 0$ for fixed, non-zero $\frac{\bar{R}}{S}$.

It is less straightforward to relate the lift due to wing-body angle, $\alpha_W - \alpha_B$, expressed by $J\left(\beta, \frac{R}{S}\right)$, to that acting in the symmetrical case, since $J\left(\frac{1}{2}, \frac{R}{S}\right)$ tends to zero as $R \to S$ (Fig.7). Instead, the function $J\left(\beta, \frac{R}{S}\right)$, evaluated numerically, is itself considered and this is tabulated in Table 3 and plotted in Fig.9 for various values of β. Note that Fig.9, like Fig.8, uses $\frac{R}{S}$ and $\frac{S}{R}$ as variables in the same chart. Once again, for each value of $\frac{R}{S}$ the effect of asymmetry increases monotonically with β. The effect is small until the wing approaches the extreme position and would be smaller still in terms of $\frac{\bar{R}}{S}$, since the points where the curves of Fig.9 run into the axis on the right are all at $\frac{\bar{R}}{S} = 1$. As in the case of common incidence, the effect of asymmetry vanishes as $\frac{R}{S} \to 0$ and as $\frac{\bar{R}}{S} \to 1$, as would be expected. The significance of the results shown in Fig.9 can be seen in the simple case of a slender wing at incidence with a circular cylinder at zero incidence, with diameter equal to the wing span, just making contact with the wing at the mid-point of its trailing edge. This corresponds to $\beta = 0$, $\frac{R}{S} = 1$ and it can be seen that the body reduces the lift slope of the wing from 2π to 3.92, i.e. by 38%. By contrast, Fig.8 shows that the lift slope of the combination, when the body incidence changes with that of the wing, is 27% greater than that of the wing alone. For values of $\frac{R}{S}$ different from 1, Fig.8 shows the increase in the lift slope of an asymmetrically mounted wing-body combination over that of a wing and a symmetrically mounted body. For the same configuration as that just considered, the effects of the asymmetry is still fairly substantial for an $\frac{R}{S}$ of 0.5, the increase in the lift slope being 10%. Its value continues to fall as $\frac{R}{S}$ gets smaller; in particular for an $\frac{R}{S}$ of 0.25, it is only 1% greater than for the symmetric configuration.

5.2 Lift and moment in a particular case

Since the effects of asymmetry on pitching moment are likely to be more significant than those on lift alone, it seems reasonable to ask how the calculated effect of the asymmetry would affect the design of a wing intended to produce a given pitching moment, for instance, to trim a supersonic transport aircraft. Consider a combination of a 60° delta wing and a body which, over the length of the wing, is a circular cylinder of diameter equal to one-sixth of the wing span. Suppose that the wing is to be mounted low on the body at the trailing edge, perhaps to let the wing structure pass below the cabin floor. Suppose that, at the cruising condition, a lift coefficient of 0.1, based on gross wing area, is to be produced with the fuselage at zero incidence. Then the present results yield at once the incidence of the wing, and so the wing body angle, at the trailing edge. If in addition the configuration must produce a pitching moment at zero lift, based on the centre-line chord of the gross wing, of 0.014*, by means of parabolic lengthwise camber of the wing, the present theory enables the amount of camber to be determined. The calculation is described in Appendix 5. It emerges that the centre section of the gross wing would need 1.05% of negative camber, bringing the apex of the gross wing to a point 20.3% of the body radius below the centre-line of the body. The aerodynamic centre of the resulting configuration is 67.25% of the centre-line chord from the

---

* This is twice the moment needed to shift the centre of pressure at $C_L = 0.1$ forward by 7% of the centre-line chord from the aerodynamic centre. 7% is a typical shift of aerodynamic centre between the most forward position at the air-field approach speed and its position at cruise at a Mach number near 2. Roughly twice as much lengthwise camber is needed to produce a given zero-lift pitching moment at a Mach number of 2 as at a Mach number of 1, to which the slender-body theory calculations can be taken to refer.

apex of the gross wing. For comparison, the properties of this same configuration can be calculated by cruder approximations and the results used to illustrate the effect of the asymmetrical mounting of the wing on the body.

Suppose first that the asymmetry of the mounting is ignored, but the same variation of wing-body angle along the length of the configuration is maintained. Then the common incidence, α_B, at which zero overall lift is reached is somewhat less negative in the approximation, since $J\left(\frac{1}{2}, \frac{1}{6}\right)$ is substantially less than $J\left(0.1, \frac{1}{6}\right)$, whereas $G\left(\frac{1}{2}, \frac{1}{6}\right)$ is very little less than $G\left(0.1, \frac{1}{6}\right)$, as can be seen from Figs.8 and 9. Fig.11 shows the variation of the lift carried forward of a certain lengthwise station with the distance, x, of that station from the apex of the gross wing, at the attitude for which the overall lift is zero. The less negative body incidence in the approximation is reflected in the less negative fore-body lift in the figure. In spite of this greater fore-body lift, the pitching moment at zero lift as calculated in Appendix 5 is 0.012, which is less than the value of 0.014 by the full present method. This is because the effects of asymmetry in increasing the lift due to wing-body angle in the full method as compared with the approximation are greater over the forward part of the wing where $\frac{R}{S}$ is near to unity, in spite of the smaller displacement of the wing from the mid-position there. The change in C_{m_0} is therefore a resultant of opposing factors and is a typical change rather than a maximum. Ignoring the asymmetry of the mounting also produces a small change in the position of the aerodynamic centre, moving it 0.15% aft to 67.4% of the centre-line chord from the apex of the gross wing. This is entirely due to the change from $G\left(\beta, \frac{R}{S}\right)$ to $G\left(\frac{1}{2}, \frac{R}{S}\right)$, where β varies from 0.565* to 0.9 from the front to the rear of the gross wing, while $\frac{R}{S}$ falls to $\frac{1}{6}$ at the trailing edge. Once again, it is over the forward part of the exposed wing, where $\frac{R}{S}$ is close to one, that the effects of asymmetry are most pronounced, in spite of the more symmetrical mounting there.

A further approximation is to ignore the presence of the body entirely. This leads, of course, to a very much larger pitching moment at zero lift, $C_{m_0} = 0.0255$, as would be expected both from the effect of wing-body angle in reducing the local incidence of the configuration below that of the wing which it covers and from the reduced lifting efficiency of a wing-body combination at a common incidence below that of a wing alone, shown in Fig.7. The aerodynamic

* For the particular case, the mid-point of the wing section is below the corresponding point on the body centre-line, in a given cross-flow plane, which corresponds to negative values of (h - g). However, since the lift is an even function of (h - g) (Section 2), and since in addition, $\beta = \frac{1}{\pi} \cos^{-1} \frac{(h-g)}{R}$, we can use the relation $L(1 - \beta) \equiv L(\beta)$.

centre of the wing alone is at $\frac{2}{3}$ of the wing length from the apex, showing that the addition of the body reduced the lifting efficiency rather more over the forward part where $\frac{R}{S}$ is near unity than over the rear where it is small. Since $G\left(\frac{1}{2}, \frac{R}{S}\right)$ is the same for $\frac{R}{S}$ zero and unity, this is again the resultant of opposing tendencies.

When the configuration is reduced to the wing alone, the effects of Mach number can be assessed by supersonic linearized theory, the calculations carried out by slender-body theory then representing the situation at sonic speed. In Appendix 5, the pitching moment of the wing alone at zero lift is calculated for a Mach number of 2, at which the wing leading edges are just sonic. The value found is 0.0108. This is less than half that at a Mach number of 1, a change which should emphasize one of the obstacles mentioned in the introduction to the indiscriminate application of the present results, derived as they are by slender-body theory. It is tempting to suppose that the reductions in C_{m_o} from the wing alone value at M = 1 to the wing alone value at M = 2 and to the wing-body combination at M = 1 could be superimposed, giving an overall reduction factor of about 4 for the wing-body combination at M = 2. However it seems likely that slender-body theory would tend to over-estimate somewhat the effects of wing-body interference in inviscid flow and, in any case, there can be no justification for superimposing such large corrections.

For uncambered configurations, the corrections are much smaller, as can be seen directly from Figs.7, 8 and 9, so that an approach on the lines of Ref.4, as suggested in the introduction, would probably be successful for lift slope and aerodynamic centre. For pitching moment and zero lift incidence of a cambered configuration, more is probably required; if the symmetrical configuration could be treated by the quasi-cylinder theory of supersonic flow, enabling the influence of Mach number to be properly assessed, then the present small correction for the effect of asymmetrical mounting could be superimposed with some degree of confidence.

6 CONCLUSIONS

(a) The lift force on a wing-body combination consisting of a slender wing with uncambered cross-sections mounted on a body whose cross-sections are circles of constant diameter over the length of the wing has been calculated by slender-body theory. Both wing and body may have arbitrary lengthwise camber. The effects of asymmetry in the mounting of the wing on the body are taken into account. The pitching moment follows by integration.

(b) The effects of the asymmetrical mounting are substantial when the body diameter is more than half of the wing span, but fall off as the body shrinks. To illustrate this a configuration has been considered consisting of a slender wing at incidence, with a circular cylinder just making contact with it at the mid-point of the trailing edge. At constant wing-body angle, the lift slope of the configuration is greater than that of the wing and the same body mounted symmetrically, by amounts 27%, 10%, and 1% for values of the ratio of body diameter to wing span of 1:1, 1:2 and 1:4 respectively. The first of these is an extreme case, but the second also shows the large effects of asymmetry. For typical aircraft configurations the pitching moment is more affected than the lift.

(c) Various combinations of factors make the direct application of the calculated results inadvisable. On the other hand, they seem likely to be useful in providing corrections to experimental or other theoretical results; for uncambered configurations they might yield corrections to results for isolated wings to make them applicable to asymmetrical wing-body combinations and for cambered configurations they might yield corrections to results for symmetrically mounted wings to allow for asymmetrical mounting.

SYMBOLS

a_1	transformation parameter (Appendix 4 only)
a_r	coefficient of $(\chi\,\bar{R})^{-r}$ in the expansion of t (Section 3)
a'_r	coefficient of $([\chi - i\,g]\bar{R})^{-r}$ in the expansion of t (Appendix 2)
b_1	coefficient of $\frac{U}{\chi}$ in the expansion of the complex potential $W(\chi)$
d	transformation parameter
$f(t)$	$\frac{d\chi}{dt}$
$g(x)$	distance of the wing below the x axis, at station x
$h(x)$	distance of the body centre-line below the x axis, at station x
$G\left(\beta, \frac{R}{S}\right)$	$L\left(\alpha_B, 0, \beta, \frac{R}{S}\right) \div \left\{\frac{1}{2}\rho\, U^2\, S^2(x)\, \alpha_B\right\}$ for $R < S$; 2π for $R \geq S$
$\tilde{G}\left(\beta, \frac{R}{S}\right)$	$G\left(\beta, \frac{R}{S}\right) \div G\left(\frac{1}{2}, \frac{R}{S}\right)$
$I\left(\beta, \frac{R}{S}\right)$	$J\left(\beta, \frac{R}{S}\right) \div \left\{16\left[\frac{\bar{R}(x)}{S(x)}\right]^2 a_1(n\,\beta + 1 - \beta)\right\}$

SYMBOLS (Continued)

$J\left(\beta, \frac{R}{S}\right)$	$L\left(0, \alpha_W - \alpha_B, \beta, \frac{R}{S}\right) \div \left\{\frac{1}{2} \rho U^2 S^2(x) (\alpha_W - \alpha_B)\right\}$
$L\left(x; \alpha_B, \alpha_W - \alpha_B, \beta, \frac{R}{S}\right)$, $L\left(\alpha_B, \alpha_W - \alpha_B, \beta, \frac{R}{S}\right)$, $L(x)$	lift force acting forward of the station x. Shorter versions used where no ambiguity exists
ℓ	centre-line chord of gross wing (Appendix 5)
n	transformation parameter
n	outward drawn normal (Appendix 1 and Section 2)
p	complex variable in transformed plane
$R(x)$	fuselage radius at station x
$\bar{R}(x)$	$R(x) \sin \beta\pi$
S	area of wing (Appendix 5)
s	length along contour (Appendix 1)
$S(x)$	wing semi-span at station x
S_1	transformation parameter
t	complex variable function in the second transformed plane - general case
U	free stream velocity
V_n, V'_n	velocity components normal to the boundary in χ, χ' planes
$W(\chi)$	complex potential in the cross-flow plane
x, y, z	right handed Cartesian co-ordinates; origin at body nose, Ox in stream direction, Oy to starboard
α	local wing or fuselage incidence
β	wing height parameter (Fig.1)

SYMBOLS (Continued)

ε	variable used in Appendix 2
λ, μ	integration variables
λ_o, μ_o, ν_o	functions of $\frac{R}{S}$ (Appendix 4)
ρ	density
ζ	complex variable function in first transformed plane
ϕ	velocity potential
ψ	stream function
χ	complex variable in the cross-flow plane

Suffices

B	body
G	body centre
T	trailing edge
W	wing

REFERENCES

No.	Author	Title, etc.
1	Pepper, P.A.	Minimum induced drag in wing-fuselage interference. NACA Tech. Note No.812, ARC.5434, September 1941.
2	Dugan, D.W., Hikido, K.	Theoretical investigation of the effects upon lift of a gap between wing and body of a slender wing-body combination. NACA Tech. Note No.3224, August 1954.
3	Stocker, P.	Supersonic flow past bodies of revolution with thin wings of small aspect ratio. Aeronautical Quarterly, 3, p.61, May 1951.
4	Pitts, W.C., Nielsen, J.N., Kaattari, G.E.	Lift and centre of pressure of wing-body-tail combinations at subsonic, transonic and supersonic speeds. NACA Report No.1307, 1957.

REFERENCES (Continued)

No.	Author	Title, etc.
5	Ward, G.N.	Linearised theory of high speed flow. Cambridge University Press, 1955.
6	Heaslet, M.A., Lomax, H.	Supersonic and transonic small perturbation theory. Section D of General Theory of High Speed Aerodynamics (Ed. Sears). Oxford University Press, London, 1955.

APPENDIX 1

THE LATERAL FORCE ON A SLENDER BODY EXPRESSED IN TERMS OF THE COMPLEX POTENTIAL

The relation (35) derived in this Appendix has been given by Ward[5], equation (9.7.11). The present amplification of his analysis is thought to be useful in view of the importance of the result and the difficulty experienced in following the steps of the argument.

We start with his expression (9.7.1) for the vectorial lateral force acting on that point of a slender body forward of a cross-flow plane:

$$\underline{F} = \rho\, \underline{U} \wedge \int_C \phi \, d\underline{s} \qquad (30)$$

where C is the contour bounding the base of the body in the cross-flow plane and the contour is described in the clockwise sense while looking upstream. The sense of description of the contour follows from the derivation of (9.7.1) in (4.6.15). Writing the vectors in their Cartesian components, we have

$$\underline{j}\, F_y + \underline{k}\, F_z = \rho\, U \int_C \phi(\underline{k}\, dy - \underline{j}\, dz)$$

with the same sense of description. Hence for the complex lateral force,

$$F = F_y + i\, F_z = -i\, \rho\, U \int_C \phi(dy + i\, dz)$$

where the contour is now in the conventional positive sense of complex variable theory, that is anti-clockwise while looking upstream. Then, in terms of the complex variable $\chi = y + i\, z$, and the complex potential $W = \phi + i\, \psi$

$$F = -i\, \rho\, U \int_C W\, d\chi - \rho\, U \int_C \psi\, d\chi \ . \qquad (31)$$

Now, W has no singularities outside C and it can be made single-valued by introducing a cut extending from C to the point at infinity. For large values of χ it can be expanded in the form

$$\frac{W}{U} = \frac{1}{2\pi} S'(x) \log \chi + b_o + \frac{b_1}{\chi} + \frac{b_2}{\chi^2} + \ldots\ldots$$

where $S(x)$ is the cross-sectional area of the slender body. This expansion converges for all points χ which are further from the origin than the furthermost singularity of W and therefore it converges for at least one point, χ_o, of C. Choose the cut in the χ plane to join χ_o to infinity. Consider another contour C_1 which passes through χ_o and surrounds C and is so chosen that the expansion of W converges on its whole length. Then W is analytic and one valued between C and C_1 and so

$$\int_C W \, d\chi = \int_{C_1} W \, d\chi$$

$$= U \int_{C_1} \left\{ \frac{1}{2\pi} S'(x) \log \chi + b_o + \frac{b_1}{\chi} + \frac{b_2}{\chi^2} + \ldots\ldots \right\} d\chi$$

$$= \frac{U}{2\pi} S'(x) \, 2\pi i \, \chi_o + 2\pi i \, b_1 \, U \quad .$$

We can write $\psi = \frac{U}{2\pi} S'(x) \, \theta$ + a single-valued function, where $\theta = \arg \chi$. Hence, using the Cauchy-Riemann relations,

$$\int_C \psi \, d\chi = [\psi \, \chi]_c - \int_C \chi \frac{\partial \psi}{\partial s} \, ds$$

$$= U \, S'(x) \, \chi_o - \int_C \chi \frac{\partial \phi}{\partial n} \, ds \qquad (33)$$

where n is the outward normal to C. The last integral is reduced by using the body boundary condition:

$$\frac{\partial \phi}{\partial n} = U \frac{\partial R}{\partial x} \sin \phi = U \frac{\partial R}{\partial x} R \frac{d\theta}{ds}$$

where $R = R(x, \theta) = |\chi|$ on C and ϕ is the angle between the tangent and the radius vector. Consider the streamwise rate of change of the first moment of the area $S(x)$ about the real and imaginary axis, i.e.

$$\frac{d}{dx}\left(\chi_g(x)\; S(x)\right) = \frac{d}{dx}\left\{\int_0^{2\pi}\int_0^{R(x,\theta)} \chi\; r\; dr\; d\theta\right\}$$

$$= \int_0^{2\pi} \chi\; R\, \frac{\partial R}{\partial x}\, d\theta$$

$$= \frac{1}{U}\int_C \chi\, \frac{\partial \phi}{\partial n}\, ds \qquad (34)$$

where χ_g is the position of the centre of area of the cross-section bounded by C. Substitution of equation (34) into (33), and of equations (33) and (32) into (31) leads to the result that

$$F = -i\,\rho\, U\left(\frac{U}{2\pi}\, S'(x)\; 2\pi i\; \chi_o + 2\pi i\; b_1\; U\right) - \rho\, U\left\{U\; S'(x)\; \chi_o - U\, \frac{d}{dx}\left(\chi_g(x)\; S(x)\right)\right\}$$

that is

$$F = \rho\, U^2\left[2\pi i + \frac{d}{dx}\left\{\chi_g(x)\; S(x)\right\}\right] \; . \qquad (35)$$

APPENDIX 2

EVALUATION OF THE COEFFICIENTS a_1, a_2 AND a_3, IN THE EXPANSION OF THE COMPLEX VARIABLE t FOR LARGE VALUES OF χ

We write equation (14) in the form

$$t = i\,S_1 + \varepsilon, \quad \varepsilon = \sum_{1}^{\infty} a_n \left(\frac{\bar{R}}{\chi}\right)^n .$$

We can expand the terms on the right hand side of equation (10) as follows:

$$\log\left(\frac{n+t}{n-t}\right) = \log\left(\frac{n+i\,S_1}{n-i\,S_1}\right) + \frac{2n\,\varepsilon}{n^2+S_1^2} + \frac{2i\,n\,S_1\,\varepsilon^2}{(n^2+S_1^2)^2} + \frac{2n(n^2-3S_1^2)\,\varepsilon^3}{(n^2+S_1^2)^3} + O(\varepsilon^4)$$

$$\log\left(\frac{t+1}{t-1}\right) = \log\left(\frac{i\,S_1+1}{i\,S_1-1}\right) + \frac{2\varepsilon}{1+S_1^2} + \frac{2i\,S_1\,\varepsilon^2}{(1+S_1^2)^2} + \frac{2(1-3S_1^2)\,\varepsilon^3}{(1+S_1^2)^3} + O(\varepsilon^4) .$$

Using equation (13A), we find equation (10) becomes

$$\zeta = 2\left(\frac{n\,\beta}{n^2+S_1^2} + \frac{1-\beta}{1+S_1^2}\right)\varepsilon + 2i\,S_1\left(\frac{n\,\beta}{(n^2+S_1^2)^2} + \frac{1-\beta}{(1+S_1^2)^2}\right)\varepsilon^2$$

$$+ \frac{2}{3}\left(\frac{n\,\beta(n^2-3S_1^2)}{(n^2+S_1^2)^3} + \frac{(1-\beta)\,(1-3S_1^2)}{(1+S_1^2)^3}\right)\varepsilon^3 + O(\varepsilon^4) .$$

Expanding the value of ζ in equation (9) for large values of χ, we have:

$$\zeta = \frac{2\bar{R}}{\chi} - \frac{2i\,g\,\bar{R}}{\chi^2} + \frac{2\bar{R}(\bar{R}^2-3g^2)}{3\chi^3} + O(\chi^{-4}) .$$

We now equate the coefficients of powers of χ in the two expressions for ζ.

$$1 = \left(\frac{n\,\beta}{n^2 + S_1^2} + \frac{1 - \beta}{1 + S_1^2}\right) a_1$$

$$-\frac{i\,g}{\bar{R}} = \left(\frac{n\,\beta}{n^2 + S_1^2} + \frac{1 - \beta}{1 + S_1^2}\right) a_2 + i\ S_1\left(\frac{n\,\beta}{(n^2 + S_1^2)^2} + \frac{1 - \beta}{(1 + S_1^2)^2}\right) a_1^2$$

and

$$\frac{1}{3}\left(1 - \frac{3g^2}{\bar{R}^2}\right) = \left(\frac{n\,\beta}{n^2 + S_1^2} + \frac{1 - \beta}{1 + S_1^2}\right) a_3 + 2i\ S_1\left(\frac{n\,\beta}{(n^2 + S_1^2)^2} + \frac{1 - \beta}{(1 + S_1^2)^2}\right) a_1\ a_2$$

$$+ \frac{1}{3}\left(\frac{n\,\beta(n^2 - 3S_1^2)}{(n^2 + S_1^2)^3} + \frac{(1 - \beta)\ (1 - 3S_1^2)}{(1 + S_1^2)^3}\right) a_1^3 \quad .$$

These three equations can be solved in turn for a_1, a_2 and a_3. The combination of a_1, a_2 and a_3 which is required to determine the lift is (equation (23))

$$\frac{a_3}{a_1} - \frac{a_2^2}{a_1^2} + \frac{a_1^2}{4S_1^2} \quad .$$

Since this is the coefficient of $\frac{1}{\chi}$ in the expansion of an analytic function of χ, regular at infinity, it has the same value as the coefficient of $\frac{1}{\chi'}$, in the expansion in powers of $\chi'(= \chi + i\ g)$. Therefore it is identical to

$$\frac{a_3'}{a_1'} - \frac{a_2'^2}{a_1'^2} + \frac{a_1'^2}{4S_1^2}$$

where a_1', a_2' and a_3' are the solutions of the above equations with g put equal to zero. They are

$$a_1' = \left(\frac{n\,\beta}{n^2 + S_1^2} + \frac{1-\beta}{1+S_1^2}\right)^{-1}$$

$$a_2' = -i\,S_1\left(\frac{n\,\beta}{(n^2 + S_1^2)^2} + \frac{1-\beta}{(1+S_1^2)^2}\right)\Bigg/\left(\frac{n\,\beta}{n^2 + S_1^2} + \frac{1-\beta}{1+S_1^2}\right)^3$$

$$a_3' = \frac{1}{3}\left(\frac{n\,\beta}{n^2 + S_1^2} + \frac{1-\beta}{1+S_1^2}\right)^{-1} - 2S_1^2\left(\frac{n\,\beta}{(n^2 + S_1^2)^2} + \frac{1-\beta}{(1+S_1^2)^2}\right)^2\Bigg/\left(\frac{n\,\beta}{n^2 + S_1^2} + \frac{1-\beta}{1+S_1^2}\right)^5$$

$$- \frac{1}{3}\left\{\frac{n\,\beta(n^2 - 3S_1^2)}{(n^2 + S_1^2)^3} + \frac{(1-\beta)\,(1-3S_1^2)}{(1+S_1^2)^3}\right\}\Bigg/\left(\frac{n\,\beta}{n^2 + S_1^2} + \frac{1-\beta}{1+S_1^2}\right)^4 .$$

We have, therefore,

$$\frac{a_3}{a_1} - \frac{a_2^2}{a_1^2} + \frac{a_1^2}{4S_1^2} = \frac{a_3'}{a_1'} - \frac{a_2'^2}{a_1'^2} + \frac{a_1'^2}{4S_1^2}$$

$$= \frac{1}{3} - S_1^2\left[\frac{n\,\beta}{(n^2 + S_1^2)^2} + \frac{1-\beta}{(1+S_1^2)^2}\right]^2\left[\frac{n\,\beta}{n^2 + S_1^2} + \frac{1-\beta}{1+S_1^2}\right]^{-4}$$

$$- \frac{1}{3}\left[\frac{n\,\beta(n^2 - 3S_1^2)}{(n^2 + S_1^2)^3} + \frac{(1-\beta)\,(1-3S_1^2)}{(1+S_1^2)^3}\right]\left[\frac{n\,\beta}{n^2 + S_1^2} + \frac{1-\beta}{1+S_1^2}\right]^{-3}$$

$$+ \frac{1}{4S_1^2}\left[\frac{n\,\beta}{n^2 + S_1^2} + \frac{1-\beta}{1+S_1^2}\right]^{-2} .$$

APPENDIX 3

REDUCTION OF THE GENERAL EXPRESSION FOR LIFT TO A KNOWN FORM FOR THE SYMMETRICAL MOUNTING

When the wing is mounted symmetrically on the fuselage we have

$$\beta = \frac{1}{2} \quad \text{and} \quad \bar{R} = R \ .$$

We can deduce the value of the parameters d, n and S_1 from equations (11), (12) and (13), namely $d = \left(\frac{S}{R}\right)$, $n = \left(\frac{S}{R}\right)^2$ and $S_1 = \left(\frac{S}{R}\right)$. From Appendix 2 we can show that

$$a_1 = n + 1 = \left(\frac{S}{R}\right)^2 + 1$$

and

$$\frac{a_3}{a_1} - \frac{a_2^2}{a_1^2} + \frac{a_1^2}{4S_1^2} = \frac{n^2 + 1}{2n} = \frac{\left(\frac{S}{R}\right)^4 + 1}{2\left(\frac{S}{R}\right)^2} \ .$$

The corresponding expression for lift is obtained from equation (23):

$$\frac{L(x)}{\frac{1}{2}\rho\ U^2\ S^2} = 2\pi\ \alpha_B\left[1 - \left(\frac{R}{S}\right)^2 + \left(\frac{R}{S}\right)^4\right] + (\alpha_W - \alpha_B)\ J\left(\frac{1}{2}\ ,\ \frac{R}{S}\right)$$

where

$$J\left(\frac{1}{2}\ ,\ \frac{R}{S}\right) = 8\left(\frac{R}{S}\right)^2\left[1 + \left(\frac{S}{R}\right)^2\right]^2 I\left(\frac{1}{2}\ ,\ \frac{R}{S}\right) \ . \qquad (36)$$

Since $S_1 = d$ and $n = d^2$, equation (22) can be written in this particular case as

$$I\left(\frac{1}{2}, \frac{R}{S}\right) = \int_1^{d^2} \frac{2d(d^2 - \lambda^2)\, d\lambda}{[\sqrt{(d^2+\lambda)(\lambda+1)} - \sqrt{(d^2-\lambda)(\lambda-1)}]^2 \sqrt{(d^4-\lambda^2)(\lambda^2-1)}\,(\lambda^2+d^2)}$$

which reduces to

$$I\left(\frac{1}{2}, \frac{R}{S}\right) = \int_1^{d^2} d(1+d^2) \frac{(d^2-\lambda^2)\,\lambda\, d\lambda}{\sqrt{(d^4-\lambda^2)(\lambda^2-1)}\,(d^2+\lambda^2)^3} + \int_1^{d^2} \frac{d(d^2-\lambda^2)\, d\lambda}{(d^2+\lambda^2)^3}$$

where $d = \frac{S}{R}$.

The second integral is evaluated by splitting the interval $[1, d^2]$ into the two intervals, $[1, d]$ and $[d, d^2]$, and by substituting $\mu = \frac{d^2}{\lambda}$ in the second. This integral then becomes

$$\int_1^d \frac{(d^2-\mu^2)^2\, d\mu}{d(d^2+\mu^2)^3} = \frac{1}{d}\int_1^d \left\{\frac{i}{4d}\left(\frac{1}{\mu+id} - \frac{1}{\mu-id}\right) + \frac{1}{4}\left[\frac{1}{(\mu+id)^2} + \frac{1}{(\mu-id)^2}\right.\right.$$

$$\left.\left. + \frac{id}{2}\left[\frac{1}{(\mu-id)^3} - \frac{1}{(\mu+id)^3}\right]\right]\right\} d\mu \quad .$$

Its value is

$$\frac{1}{2d^2}\left(\frac{\pi}{4} - \tan^{-1}\frac{R}{S}\right) + \frac{1-d^2}{2d(1+d^2)^2} = \frac{1}{2}\left(\frac{R}{S}\right)^2\left(\frac{\pi}{4} - \tan^{-1}\frac{R}{S}\right) + \frac{1}{2}\left(\frac{R}{S}\right)^3\left\{\frac{\left(\frac{R}{S}\right)^2 - 1}{\left[\left(\frac{R}{S}\right)^2 + 1\right]^2}\right\}. \quad \ldots\ldots(37)$$

In the first integral we substitute $x^2 = \frac{\lambda^2 - 1}{d^4 - \lambda^2}$ which reduces it to the form

$$\frac{1}{2}\frac{d(d^2-1)}{(d^2+1)^2}\int_{-\infty}^{\infty} \frac{(1-d^2x^2)(1+x^2)\, dx}{(1+d^2x^2)^3} \quad .$$

Consider the contour integral

$$I_{(R)} = \oint_{C(R)} \frac{(1 - d^2 z^2)(1 + z^2)\, dz}{(1 + d^2 z^2)^3}$$

where the contour $C(R)$ is the part of the real axis $z = x$ for which $-R \leqslant x \leqslant +R$ and the semicircle $z = Re^{i\theta}$, $0 \leqslant \theta \leqslant \pi$.

We notice that the only pole within the contour lie at the point $z = \frac{i}{d}$. The residue of the integrand at this point is $-\frac{i}{8d}\left(1 - \frac{1}{d^2}\right)$. Moreover the integrand is of order (R^{-2}) for $z = Re^{i\theta}$, so

$$\lim_{R\to\infty}[I_{(R)}] = \frac{1}{2} \cdot \frac{d(d^2 - 1)}{(d^2 + 1)^2} \cdot 2\pi i\left\{-\frac{i}{8d}\left(1 - \frac{1}{d^2}\right)\right\}$$

$$= \frac{\pi}{8}\left(\frac{R}{S}\right)^2 \left\{\frac{\left(\frac{R}{S}\right)^2 - 1}{\left(\frac{R}{S}\right)^2 + 1}\right\}^2 .$$

Combining the results of equations (26), (27) and this contour integral the expression for the lift reduces to

$$\frac{L(x)}{\frac{1}{2}\rho U^2 S^2} = 2\pi \alpha_B\left[1 - \left(\frac{R}{S}\right)^2 + \left(\frac{R}{S}\right)^4\right] + 2(\alpha_W - \alpha_B)\left[\pi\left\{1 + \left(\frac{R}{S}\right)^4\right\} - 2\left(\frac{R}{S}\right)\left\{1 - \left(\frac{R}{S}\right)^2\right\}\right.$$

$$\left. -2\left\{1 + \left(\frac{R}{S}\right)^2\right\}^2 \tan^{-1}\frac{R}{S}\right] . \qquad (38)$$

This is the expression given by Dugan and Hikido.

APPENDIX 4

THE LIMITING CASE $\beta = 0$ BY AN INDEPENDENT TRANSFORMATION

When the wing-body angle is non-zero it has not proved possible to evaluate the appropriate limit of the expression for lift as $\beta \to 0$. However, this limiting configuration can be treated by an independent transformation, as follows.

Fig.4 shows the contour in the cross flow plane $\chi = y + iz$. The function

$$\zeta = \frac{R^2}{\chi - iR}$$

has zero imaginary part on the wing and constant imaginary part on the fuselage, so this relation transforms the right-hand half of the χ-plane outside the contour of Fig.4 onto the ζ-plane inside the polygonal contour of Fig.5. The appropriate Schwartz-Christoffel transformation of the interior of this polygon onto the upper half of the p-plane (Fig.6) is given by:

$$\frac{dp}{d\zeta} = k(p - a_4)^{\frac{1}{2}} (p - a_3)^{\frac{3}{2}} (p - a_2)^{-1} (p - a_1) \quad .$$

The three arbitrary constants introduced by the transformation are determined by making A_5 become the point at infinity and by setting $a_3 = -1$ and $a_4 = +1$. The conditions that the required points should correspond give the relations

$$a_2 = \frac{a_1 \cos^{-1} a_1 - \sqrt{1 - a_1^2}}{\cos^{-1} a_1 + \sqrt{1 - a_1^2}}$$

and

$$k = \frac{2\pi i}{R(\cos^{-1} a_1 + \sqrt{1 - a_1^2})} \quad .$$

The transformation is then given by

$$\frac{R^2}{\chi - iR} = \zeta = \frac{iR}{2\pi} \left\{ \cos^{-1}\left(\frac{a_1 p - 1}{p - a_1}\right) - \sqrt{\frac{p - 1}{p + 1}} \cos^{-1} a_1 \right\} \qquad \ldots.(39)$$

where a_1 is related to $\frac{R}{S}$ by

$$2\pi\frac{R}{S} = \cosh^{-1}\left\{1 + \sqrt{\frac{1-a_1}{1+a_1}}\cos^{-1} a_1\right\} + \left\{\left(1 + \sqrt{\frac{1-a_1}{1+a_1}}\cos^{-1} a_1\right)^2 - 1\right\}^{\frac{1}{2}} . \qquad \ldots.(40)$$

Equations (39) and (40) determine the transformation of the right-hand half of the χ-plane outside the contour of Fig.4 onto the upper half of the p-plane of Fig.6, with corresponding points as shown.

As in Section 2, we simplify the fuselage boundary condition by superimposing a uniform cross-flow parallel to the imaginary axis. Let

$$\phi^* = \phi + U\, z\, h'(x)$$

so that the boundary conditions become

$$\phi^*_n = 0 \text{ on the fuselage}$$

$$\phi^*_n = \mp U(\alpha_W(x) - \alpha_B(x)) \text{ on the upper and lower surfaces of the wing}$$

and

$$\phi^* \sim U\, z\, h'(x) \text{ at infinity} .$$

As before, we introduce the complex potentials W and W*, related by

$$W^* = W - U\, i\, \chi\, h'(x)$$

so that ϕ and ϕ^* are the real parts of W and W*, and we construct W* in the p-plane. For large p, χ is large and so

$$W^* \sim -U\, i\, \chi\, h'(x) = -U\, i\, \chi\, \alpha_B(x).$$

By expanding the expressions in equation (39) for large p and χ, we have:

$$p = \frac{i}{2\pi R}\left(\cos^{-1} a_1 + \sqrt{1 - a_1^2}\right)\chi + \text{constant}$$

$$+ \frac{1}{2}\pi\, iR \,\frac{\left(a_1\sqrt{1 - a_1^2} - \cos^{-1} a_1\right)^2 - 2\left(\cos^{-1} a_1 + \sqrt{1 - a_1^2}\right)\left(\cos^{-1} a_1 + \frac{1}{3}\sqrt{1 - a_1^2}\,[1 + 2a_1^2]\right)}{\left(\cos^{-1} a_1 + \sqrt{1 - a_1^2}\right)^2}$$

$$+ O(\chi^{-2}) \qquad (41)$$

and so for large p

$$W^* \sim - \frac{2\pi R\, U\, \alpha_B(x)}{\cos^{-1} a_1 + \sqrt{1 - a_1^2}}\, p \quad .$$

On the real axis in the p-plane the normal velocity is zero except on A_3A_2 and A_2A_1, where it takes the values $\mp U(\alpha_W - \alpha_B)\ \left|\frac{d\chi}{dp}\right|$ respectively. Hence we can write the complex potential at a point p_o as

$$W^*(p_o) = - \frac{2\pi R\, U\, \alpha_B}{\cos^{-1} a_1 + \sqrt{1 - a_1^2}}\, p_o + \frac{U(\alpha_W - \alpha_B)}{\pi}\left\{\int_{-1}^{a_2} - \int_{a_2}^{a_1}\left[\left|\frac{d\chi}{dp}\right| \log(p_o - p)\, dp\right]\right\}$$

since the first term produces no normal velocity on the real axis and second term produces no flow at infinity.

Since $\frac{d\chi}{dp}$ is given by

$$\frac{d\chi}{dp} = \frac{d\chi}{d\zeta}\cdot\frac{d\zeta}{dp} = \frac{R^3}{2\pi\,\zeta^2}\cdot\frac{(p - a_2)\left(\cos^{-1} a_1 + \sqrt{1 - a_1^2}\right)}{(p - a_1)\,(p + 1)^{\frac{3}{2}}\,(1 - p)^{\frac{1}{2}}} \quad .$$

We have, for $-1 \leqslant p \leqslant a_2$

$$\left|\frac{d\chi}{dp}\right| = \frac{d\chi}{dp}$$

and for $a_2 \leqslant p \leqslant a_1$

$$\left|\frac{d\chi}{dp}\right| = -\frac{d\chi}{dp}$$

since ζ is real for $-1 \leqslant p \leqslant a_1$. Hence we can write

$$W^*(p_o) + \frac{2\pi R\ U\ \alpha_B}{\cos^{-1} a_1 + \sqrt{1 - a_1^2}}\, p_o = \frac{U(\alpha_W - \alpha_B)}{\pi} \int_{-1}^{a_1} \frac{d\chi}{dp} \log(p_o - p)\, dp$$

$$= \frac{U(\alpha_W - \alpha_B)}{\pi} \int_{-1}^{a_1} \frac{R^2\, dp}{\zeta(p_o - p)}$$

on integrating by parts and substituting for χ in terms of ζ. Now, for $-1 \leqslant p \leqslant a_1$, equation (39) becomes

$$\zeta = -\frac{R}{2\pi}\left\{\cosh^{-1}\left(\frac{a_1\, p - 1}{p - a_1}\right) + \sqrt{\frac{1 - p}{1 + p}}\cos^{-1} a_1\right\} .$$

It follows that

$$W^*(p_o) = -\frac{2\pi R\ U\ \alpha_B}{\cos^{-1} a_1 + \sqrt{1 - a_1^2}}\, p_o$$

$$-\frac{2R\ U(\alpha_W - \alpha_B)}{p_o} \int_{-1}^{a_1} \frac{dp}{\left[\cosh^{-1}\left(\frac{a_1\, p - 1}{p - a_1}\right) + \sqrt{\frac{1 - p}{1 + p}}\cos^{-1} a_1\right]} + O(p_o^{-2})$$

Hence, using equation (41), we find the coefficient of $\frac{1}{\chi}$ in the expansion of $\frac{W^*}{U}$, and therefore of $\frac{W}{U}$, to be:

$$b_1 = \frac{4\pi i\ R^2(\alpha_W - \alpha_B)}{\cos^{-1} a_1 + \sqrt{1 - a_1^2}} \int_{-1}^{a_1} \frac{dp}{\left[\cosh^{-1}\left(\frac{a_1\ p - 1}{p - a_1}\right) + \sqrt{\frac{1 - p}{1 + p}} \cos^{-1} a_1\right]}$$

$$- \frac{\pi^2 i\ R^2\ \alpha_B}{(\cos^{-1} a_1 + \sqrt{1 - a_1^2})^4} \left\{(a_1\sqrt{1 - a_1^2} - \cos^{-1} a_1)^2\right.$$

$$\left. - 2(\cos^{-1} a_1 + \sqrt{1 - a_1^2}) \left(\cos^{-1} a_1 + \frac{1}{3} \sqrt{1 - a_1^2}\ [1 + 2a_1^2]\right) \right\} . \qquad \ldots.(42)$$

By Ward's result, equation (20), the lift on the configuration is given at once. If the incidences of wing and fuselage are the same, the result can be written in closed form:

$$\frac{L\left(\alpha_B, 0, 0, \frac{R}{S}\right)}{\frac{1}{2}\rho\ U^2} =$$

$$\frac{4\pi^3\ R^2\ \alpha_B}{(\cos^{-1} a_1 + \sqrt{1 - a_1^2})^4} \left\{2(\cos^{-1} a_1 + \sqrt{1 - a_1^2}) \left(\cos^{-1} a_1 + \frac{1}{3} \sqrt{1 - a_1^2}\ [1 + 2a_1^2]\right)\right.$$

$$\left. - (a_1\sqrt{1 - a_1^2} - \cos^{-1} a_1)^2\right\} - 2\pi\ R^2\ \alpha_B \ . \qquad (43)$$

This last expression can be confirmed by taking the limit as $\beta \to 0$ of the expression (25) found in the main text for the lift on the general configuration when the wing and fuselage are at the same incidence. The steps of the reduction now follow.

The assumption that β is small leads to the result, using equations (11), (12) and (13), that

$$n = \frac{\lambda_0}{\beta} + O(1)$$

$$d = \frac{\mu_o}{\beta} + O(1)$$

$$S_1 = \frac{\nu_o}{\beta} + O(1)$$

where $\lambda_o = \nu_o \cot \frac{1}{\nu_o}$, $\mu_o = \lambda_o(1 + \lambda_o)^{-\frac{1}{2}}$ and $2\pi \frac{R}{S} = \log\left(\frac{\lambda_o + \mu_o}{\lambda_o - \mu_o}\right) + \frac{2}{\mu_o}$. The last of these can be written in terms of ν_o as

$$2\pi \frac{R}{S} = \log\left\{\frac{\sqrt{1 + \nu_o \cot \frac{1}{\nu_o}} + 1}{\sqrt{1 + \nu_o \cot \frac{1}{\nu_o}} - 1}\right\} + \frac{2\sqrt{1 + \nu_o \cot \frac{1}{\nu_o}}}{\nu_o \cot \frac{1}{\nu_o}} .$$

The expressions for a_1', a_2' and a_3', given in Appendix 2, become

$$a_1' = \left(\frac{\lambda_o}{\lambda_o^2 + \nu_o^2} + \frac{1}{\nu_o^2}\right)^{-1} \beta^{-2} + O(\beta^{-1})$$

$$a_2' = -i\,\nu_o\left[\frac{\lambda_o}{(\lambda_o^2 + \nu_o^2)^2} + \frac{1}{\nu_o^4}\right]\left[\frac{\lambda_o}{\lambda_o^2 + \nu_o^2} + \frac{1}{\nu_o^2}\right]^{-3} \beta^{-3} + O(\beta^{-2})$$

and

$$a_3' = -2\nu_o^2\left[\frac{\lambda_o}{(\lambda_o^2 + \nu_o^2)^2} + \frac{1}{\nu_o^4}\right]\left[\frac{\lambda_o}{\lambda_o^2 + \nu_o^2} + \frac{1}{\nu_o^2}\right]^{-5} \beta^{-4}$$

$$- \frac{1}{3}\left[\frac{\lambda_o^3 - 3\lambda_o \nu_o^2}{(\lambda_o^2 + \nu_o^2)^3} - \frac{3}{\nu_o^4}\right]\left[\frac{\lambda_o}{\lambda_o^2 + \nu_o^2} + \frac{1}{\nu_o^2}\right]^{-4} \beta^{-4} + O(\beta^{-3}) .$$

The expression for lift, equation (25), becomes in the limit as $\beta \to 0$

$$\frac{L(x)}{\frac{1}{2}\rho\, U^2\, S^2} = 4\pi^3\, \alpha_B\left(\frac{R}{S}\right)^2 \left\{\frac{E^2}{4\nu_o^2} - \nu_o^2\left[\frac{\lambda_o}{(\lambda_o^2 + \nu_o^2)^2} + \frac{1}{\nu_o^4}\right]^2 E^4\right.$$

$$\left. - \frac{1}{3}\, E^3\left[\frac{\lambda_o^3 - 3\lambda_o\, \nu_o^2}{(\lambda_o^2 + \nu_o^2)^3} - \frac{3}{\nu_o^4}\right]\right\} - 2\pi\left(\frac{R}{S}\right)^2 \alpha_B$$

where $E = \left(\frac{\lambda_o}{\lambda_o^2 + \nu_o^2} + \frac{1}{\nu_o^2}\right)^{-1}$.

On substitution of the value $\lambda_o = \nu_o \cot \frac{1}{\nu_o}$ into this expression we obtain

$$\frac{L(x)}{\frac{1}{2}\rho\, U^2\, S^2} = \frac{1}{3}\,\pi^3\, \alpha_B\left(\frac{R}{S}\right)^2 \left\{\frac{3\nu_o^2 \operatorname{cosec}^2 \frac{1}{\nu_o}}{E_o^2} - \frac{12\nu_o^2\left(\nu_o \cot \frac{1}{\nu_o} + \operatorname{cosec}^4 \frac{1}{\nu_o}\right)^2}{E_o^4}\right.$$

$$\left. - \frac{4\nu_o^2}{E_o^3}\left(\nu_o \cot^3 \frac{1}{\nu_o} - 3\nu_o \cot \frac{1}{\nu_o} - 3 \operatorname{cosec}^6 \frac{1}{\nu_o}\right)\right\} - 2\pi\, \alpha_B\left(\frac{R}{S}\right)^2 \qquad \ldots.(44)$$

where $E_o = \left(\nu_o \cot \frac{1}{\nu_o} + \operatorname{cosec}^2 \frac{1}{\nu_o}\right)$.

The equation relating ν_o in terms of $\frac{R}{S}$ is, as before,

$$2\pi\,\frac{R}{S} = \log\left\{\frac{\sqrt{1 + \nu_o \cot \frac{1}{\nu_o}} + 1}{\sqrt{1 + \nu_o \cot \frac{1}{\nu_o}} - 1}\right\} + \frac{2\sqrt{1 + \nu_o \cot \frac{1}{\nu_o}}}{\nu_o \cot \frac{1}{\nu_o}} \; . \qquad \ldots.(45)$$

Comparison of equations (45) and (40) produces the following relationship between the parameters ν_o and a_1:

$$\nu_o \cot \frac{1}{\nu_o} = \frac{2}{\cos^{-1} a_1} \sqrt{\frac{1 + a_1}{1 - a_1}}$$

which reduces to

$$\nu_o = \frac{2}{\cos^{-1} a_1} .$$

By substituting this value for ν_o into equation (44), we can rederive the expression for lift given in equation (43), thereby establishing the equivalence of the two methods.

APPENDIX 5

APPLICATION OF THE METHOD TO A TYPICAL SUPERSONIC TRANSPORT CONFIGURATION

We compare the results obtained from the present method with those obtained using the previously available formulae, for example, with the expression given by Stocker[3] for a symmetrically mounted wing. The use of his formulae is only strictly justified if the wing-body angle is sufficiently small for the departure from symmetrical mounting to be ignored. We compare the chordwise distributions of lift, that is, of the lift acting ahead of the chordwise station considered, and the values of $\frac{\partial C_M}{\partial C_L}$ and C_{M_o}. Similar results are included for the wing alone to see what effect the body has. The contribution of the forebody is included in the calculation of overall lift, but not for overall moments, since this would involve assuming its shape and length.

The wing was designed on the assumption of typical geometric and aerodynamic characteristics as detailed below:

(i) The wing is taken to be of delta planform, having a leading edge sweepback of 60°.

(ii) The fuselage is taken to have circular cross-sections of constant radius, equal to one sixth of the wing trailing edge semi-span. It is not cambered.

(iii) The wing is taken to have a low position on the fuselage at the trailing edge, with a wing-body angle chosen to give a C_L, based on gross wing area, of 0.1 at zero body incidence.

(iv) We assume no spanwise camber, but suitable parabolic longitudinal camber to give $C_{M_o} = 0.014$ (based on centre line chord). This is about twice the C_{M_o} that would be required for trim at $M = 2$ since there is some evidence that the effectiveness of longitudinal camber is reduced by a factor of about 2 between $M = 1$ and $M = 2$.

The first step is to use the design value of the lift coefficient, C_L, to calculate the trailing edge wing-body angle, $(\alpha_W - \alpha_B)_T$, from the third condition. Secondly the wing camber can be determined from the design value of C_{M_o}, Condition (iv).

1 Evaluation of the trailing edge wing-body angle

When $\alpha_B = 0$,

$$\frac{L\left(0,\ \alpha_W - \alpha_B,\ \beta,\ \frac{R}{S}\right)}{\frac{1}{2}\rho\ U^2\ S^2} = J\left(\beta,\ \frac{R}{S}\right)\ (\alpha_W - \alpha_B)\quad .$$

It is straightforward to calculate the value of $J\left(\beta, \frac{R}{S}\right)$, for $\beta = 0.1$ and $\frac{R}{S} = \frac{1}{6}$, from equation (24). We have

$$J\left(\beta,\ \frac{R}{S}\right) = 16\left(\frac{R}{S}\right)^2 \sin^2 \beta\pi\ a_1(n\ \beta + 1 - \beta)\ I\left(\beta,\ \frac{R}{S}\right)$$

where a_1 and $I\left(\beta, \frac{R}{S}\right)$ are given in Appendix 2 and equation (22), viz

$$a_1 = \left[\frac{n\ \beta}{n^2 + S_1^2} + \frac{1 - \beta}{1 + S_1^2}\right]^{-1}$$

and

$$I\left(\beta,\ \frac{R}{S}\right) = \int_1^n \frac{2S_1(d^2 - \lambda^2)\ d\lambda}{\{(n+\lambda)^\beta(\lambda+1)^{1-\beta} - (\lambda-1)^\beta(\lambda-1)^{1-\beta}\}^2(n^2-\lambda^2)^{1-\beta}(\lambda^2-1)^\beta(\lambda^2+S_1^2)}$$

Numerical evaluation of $I\left(0.1,\ \frac{1}{6}\right)$ produces the result that

$$J\left(0.1,\ \frac{1}{6}\right) = 5.82769\quad .$$

It follows from the definition of C_L that $(\alpha_W - \alpha_B)_T$ is given by

$$(\alpha_W - \alpha_B)_T = \frac{C_L}{J\left(0.1,\ \frac{R}{S}\right)} \cdot \frac{\ell}{S}$$

$$= 0.0297210\quad .$$

From these values of $J\left(0.1, \frac{R}{S}\right)$ and $(\alpha_W - \alpha_B)_T$, we find the body incidence for zero overall lift from equation (25). It is

$$\alpha_B = -0.0282884 \quad .$$

2 Evaluation of the longitudinal camber

We obtain the following expression for the pitching moment, M, from equation (27):

$$M = -\ell \, L(\ell) + \int_0^{\ell} L(x) \, dx$$

where x is measured now from the apex of the gross wing. Equivalently, we have

$$C_M = \frac{1}{S\ell} \left\{ \int_0^{\ell} \frac{L(x)}{\frac{1}{2}\rho \, U^2} \, dx - \ell \, \frac{L(\ell)}{\frac{1}{2}\rho \, U^2} \right\} \quad .$$

Two facts complicate the evaluation of the camber for the prescribed value of C_{M_0}. The first of these arises from the fact that values of the lift force, $L(x)$, are known only for a small but representative set of values of β and $\frac{R}{S}$, whereas these two parameters vary continuously over the length of the wing. It will be noticed from Fig.10, which records the variation of $G\left(\beta, \frac{R}{S}\right)$ and $J\left(\beta, \frac{R}{S}\right)$ with $\sin \beta\pi$ for a typical value of $\frac{R}{S}$, that the function $J\left(\beta, \frac{R}{S}\right)$ varies almost linearly with $\sin \beta\pi$. It is concluded that it is sufficiently accurate to replace the functions $J\left(\beta, \frac{R}{S}\right)$ and $G\left(\beta, \frac{R}{S}\right)$ by second and fifth order polynomials in $\sin \beta\pi$, respectively, whose coefficients are functions of $\frac{R}{S}$. The dependence of the two functions upon $\frac{R}{S}$ is apparently not so simple. The integral in the expression for C_M was evaluated using integration formulae which require the values of the functions at a number of discrete points. Expressions were found for C_M and $\frac{\partial C_M}{\partial C_L}$ using these approximations.

The second complication in the analysis arises because the value of C_{M_o} depends on the camber in a complicated fashion, involving the angle β. In fact the calculation of the required camber is easily programmed for a computer. The method adopted was to use the values of C_{M_o}, corresponding to two arbitrary amounts of camber, as a basis for an iteration procedure to calculate the camber required to give the prescribed value for C_{M_o}.

This results in the apex of the gross wing lying 20.3% of the body radius below the centre line or, equivalently, in the cross-section of the gross wing having 1.05% of negative camber.

For this configuration the values of C_{M_o} and $\frac{\partial C_M}{\partial C_L}$ were also calculated by two simpler approximations. If the displacement of the wing from the body centre-line is ignored, but the actual variation of wing-body angle is taken into account, the lift and moment can be evaluated from the formulae of Ref.2, obtained by setting $\beta = \frac{1}{2}$ in the present work. This provides the second row of the table below. The third row gives the values according to slender-body theory for the wing alone, obtained from the familiar results given by putting $\frac{R}{S} = 0$ in the present work. The final row is for the wing alone at a Mach number of 2, when the leading edge of the wing is sonic, according to linearised theory. The factor to be applied to the value of C_{M_o} at a Mach number of 1 to give the C_{M_o} at a larger Mach number, M, for which the leading edge is not yet supersonic, can be obtained from equation (13-39) of Ref.5 as

$$\frac{1 - \theta^2}{\theta^2 K + (1 - 2\theta^2)E}$$

where $\theta^2 = (M^2 - 1) \cot^2 \Lambda$, Λ = leading edge sweep and K and E are complete elliptic integrals of the first and second kind with modulus $(1 - \theta^2)^{\frac{1}{2}}$. As $\theta \to 1$, the value corresponding to M = 2, the ratio tends to $4/3\pi$.

	C_{M_o}	$\frac{\partial C_M}{\partial C_L}$	$\left(\frac{\partial C_M}{\partial C_L}\right) \Big/ \left(\frac{\partial C_M}{\partial C_L}\right)_{\text{wing alone}}$
Present method	0.0140	-0.67252	1.0088
Symmetrical mounting	0.0120	-0.67407	1.0111
Wing alone (M = 1)	0.0255	-0.66667	1
Wing alone (M = 2)	0.0108	-0.66667	1

The lift acting forward of the lengthwise station distance x from the apex of the gross wing is plotted against x in Fig.11 for the attitude of zero overall lift. The results of the present calculations are compared with those of the two simplified calculations by slender-body theory mentioned above. For the wing alone, the effect of Mach number is just that of a change of scale.

TABLE 1

The functions $J\left(\frac{1}{2}, \frac{R}{S}\right)$ and $G\left(\frac{1}{2}, \frac{R}{S}\right)$

$\frac{S}{R}$	$\frac{R}{S}$	$J\left(\frac{1}{2}, \frac{R}{S}\right)$	$G\left(\frac{1}{2}, \frac{R}{S}\right)$	$\frac{S}{R}$	$\frac{R}{S}$	$J\left(\frac{1}{2}, \frac{R}{S}\right)$	$G\left(\frac{1}{2}, \frac{R}{S}\right)$
1	1	0	2π	3.0	$\frac{1}{3}$	3.5868	5.6626
1.05263	0.95	-	5.7303	3.5	0.2857	3.9733	5.8123
1.125	0.8889	0.145	5.2415	4	0.25	4.2642	5.9150
1.25	0.8	0.4457	4.8355	4.5	0.22222	4.4902	5.9881
1.375	0.72727	0.7914	4.7181	5.0	0.2	4.6712	6.0419
1.5	0.6667	1.1356	4.7317	5.5	0.18182	4.8190	6.0828
1.1111	0.9	-	5.3162	6	0.16667	4.9421	6.1135
$\frac{5}{3}$	0.6	-	4.8355	10	0.1	5.4811	6.2210
2	0.5	2.2822	5.1051	20	0.05	5.8828	6.2675
2.5	0.4	3.0520	5.4387	100	0.01	-	6.2826

TABLE 2A

The function $\tilde{G}\left(\beta, \frac{R}{S}\right)$ for various values of β and $\frac{R}{S}$

		Values of β						
		0	0.01	0.05	0.1	0.2	0.3	0.4
Values of $\frac{R}{S}$	0.1	1.0002	1.0002	1.0002	1.0002	1.0001	1.00007	1.00002
	0.2	1.0034	1.0034	1.0034	1.0031	1.0023	1.0012	1.0004
	0.3	1.0163	1.0163	1.0159	1.0149	1.0111	1.0061	1.0017
	0.4	1.0473	1.0473	1.0463	1.0435	1.0327	1.0182	1.0052
	0.5	1.1029	1.1029	1.1009	1.0950	1.0724	1.0408	1.0119
	0.6	1.1822	1.1821	1.1789	1.1687	1.1297	1.0739	1.0217
	0.7	1.2698	1.2696	1.2649	1.2502	1.1931	1.1102	1.0324
	0.8	1.3334	1.3332	1.3273	1.3089	1.2371	1.1330	1.0379
	0.8558	1.3445	(Max value attained for β = 0)					
	0.9	1.3371	1.3368	1.3304	1.3104	1.2323	1.1222	1.0310
	1.0	1.2671	1.2669	1.2607	1.2414	1.1670	1.0691	1.0077
Values of $\frac{S}{R}$	0.98	–	–	–	–	–	–	1.0027
	0.96	–	–	–	–	–	–	1.0003
	0.95	–	–	–	1.1944	1.1245	1.0376	
	0.9	1.1765	–	–	1.1535	1.0888	1.0156	
	0.85	–	–	–	1.1185	1.0598	1.0031	
	0.8	1.1086	–	–	1.0891	1.0372		
	0.75	–	–	–	1.0650	1.0205		
	0.7	1.0610	–	–	1.0456	1.0091		
	0.65	–	–	–	1.0306	1.0026		
	0.6	1.0304	–	–	1.0193			
	0.55	–	–	–	1.0113			
	0.5	1.0128	–	–	1.0059			
	0.45	–	–	–	1.0026			
	0.40	1.0043	–	–	1.0009			
	0.35	–	–	–	1.0001			
	0.30	1.0010	–	–				
	0.20	1.0001	–	–				

TABLE 2B

The function $\tilde{G}\left(\beta, \frac{\bar{R}}{\bar{S}}\right)$ for various values of β and $\frac{\bar{R}}{\bar{S}}$

		Values of β					
		0.01	0.05	0.1	0.2	0.3	0.4
Values of $\frac{\bar{R}}{\bar{S}}$	0.1	1.0012	1.2131	1.0199	1.0012	1.0002	1.0000
	0.2	1.0000	1.0940	1.2077	1.0179	1.0028	1.0004
	0.3	1.0000	1.0137	1.2683	1.0776	1.0137	1.0022
	0.4	1.0000	1.0030	1.0752	1.1814	1.0392	1.0063
	0.5	1.0000	1.0008	1.0230	1.2421	1.0806	1.0142
	0.6	1.0000	1.0003	1.0073	1.1488	1.1226	1.0252
	0.7	1.0000	1.00011	1.0022	1.0546	1.1307	1.0354
	0.8	1.0000	1.00009	1.0006	1.0164	1.0770	1.0369
	0.9	1.0000	1.00006	1.0001	1.0029	1.0152	1.0222

TABLE 3

The function $J\left(\beta, \frac{R}{S}\right)$ for various values of β and $\frac{R}{S}$

$\frac{R}{S}$ \ β	0	0.1	0.2	0.3	0.4	0.5	0.05
0.1	6.2702	6.0254	5.8052	5.6310	5.5195	5.4811	6.1461
0.2	6.1952	5.7184	5.2923	4.9575	4.7443	4.6712	5.955
0.3	6.0361	5.3486	4.7376	4.2609	3.9598	3.8570	5.6870
0.4	5.8008	4.9275	4.1539	3.5549	3.1795	3.0520	5.3573
0.5	5.5106	4.4773	3.5631	2.8609	2.4251	2.2781	4.9862
0.6	5.1893	4.0205	2.9874	2.2027	1.7231	1.5633	4.5970
0.7	4.8571	3.5755	2.4456	1.6028	1.1026	0.9403	4.2087
0.8	4.5289	3.1548	1.9508	1.0803	0.5936	0.4457	3.8347
0.9	4.2145	2.7657	1.5113	0.6503	0.2256	0.1185	3.4833
1.0	3.9193	2.4115	1.1308	0.3239	0.0272	0	3.1587
0.4/sin $\beta\pi$	-	1.5691	-	-	-	-	-
0.5/sin $\beta\pi$	-	0.9350	-	-	-	-	-
0.6/sin $\beta\pi$	-	0.5214	1.0593	-	-	-	-
0.7/sin $\beta\pi$	-	0.2597	0.5694	-	-	-	-
0.8/sin $\beta\pi$	-	0.1036	0.2411	-	-	-	-
0.9/sin $\beta\pi$	-	0.0236	0.0574	0.0893	-	-	-
10/9	3.6172	-	-	-	-	-	2.8309
1.25	3.2785	-	-	-	-	-	2.4688
5/3	2.4941	-	-	-	-	-	1.6517
2.5	1.6029	-	-	-	-	-	0.7722
5.0	0.7119	-	-	-	-	-	-
10	0.3198	-	-	-	-	-	-

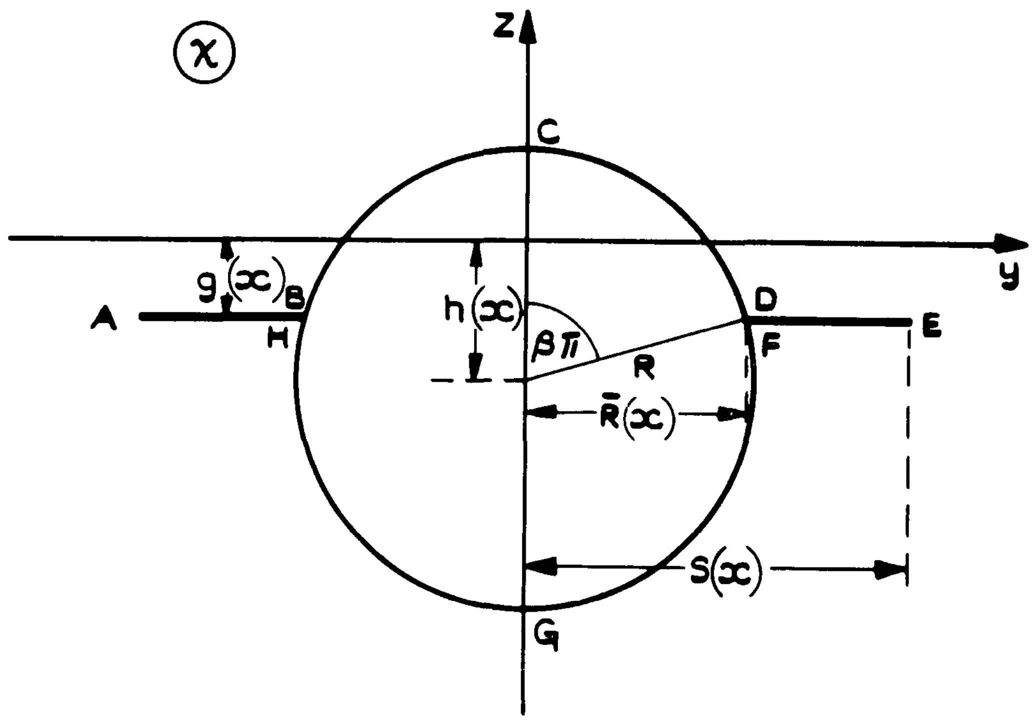

FIG. 1.(a) SECTION OF THE CONFIGURATION BY A PLANE NORMAL TO THE FREE STREAM DIRECTION.

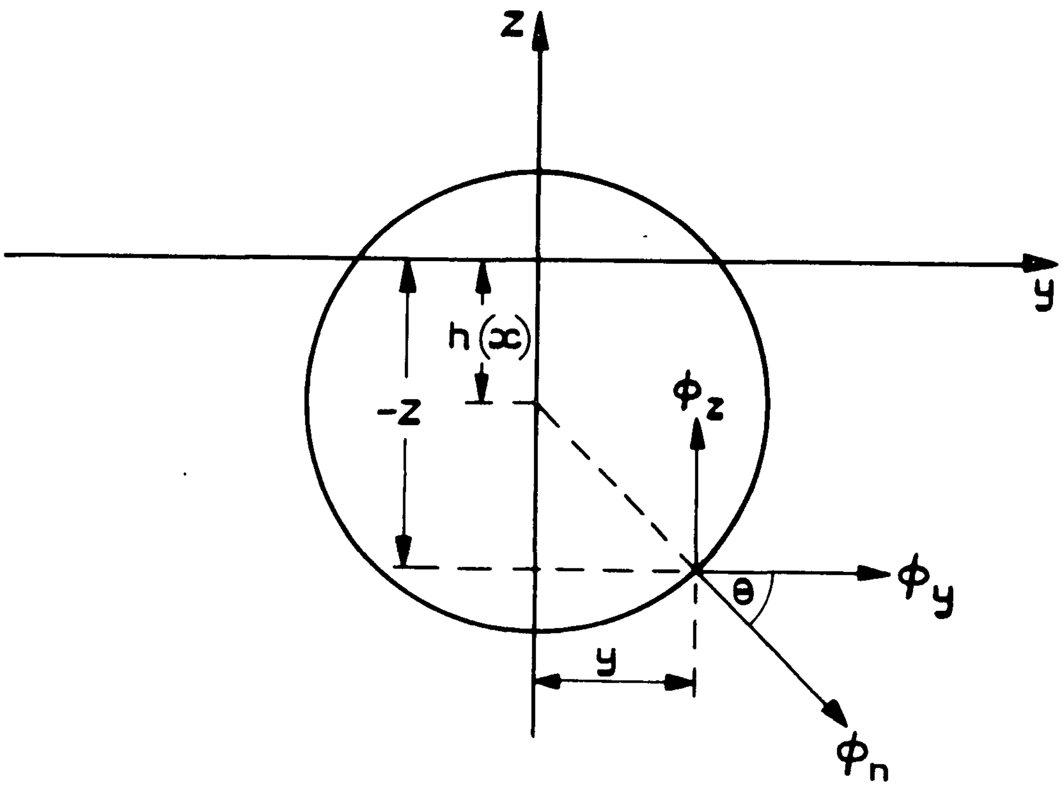

FIG. 1.(b) VELOCITY COMPONENTS IN THE PLANE OF FIG. 1(a).

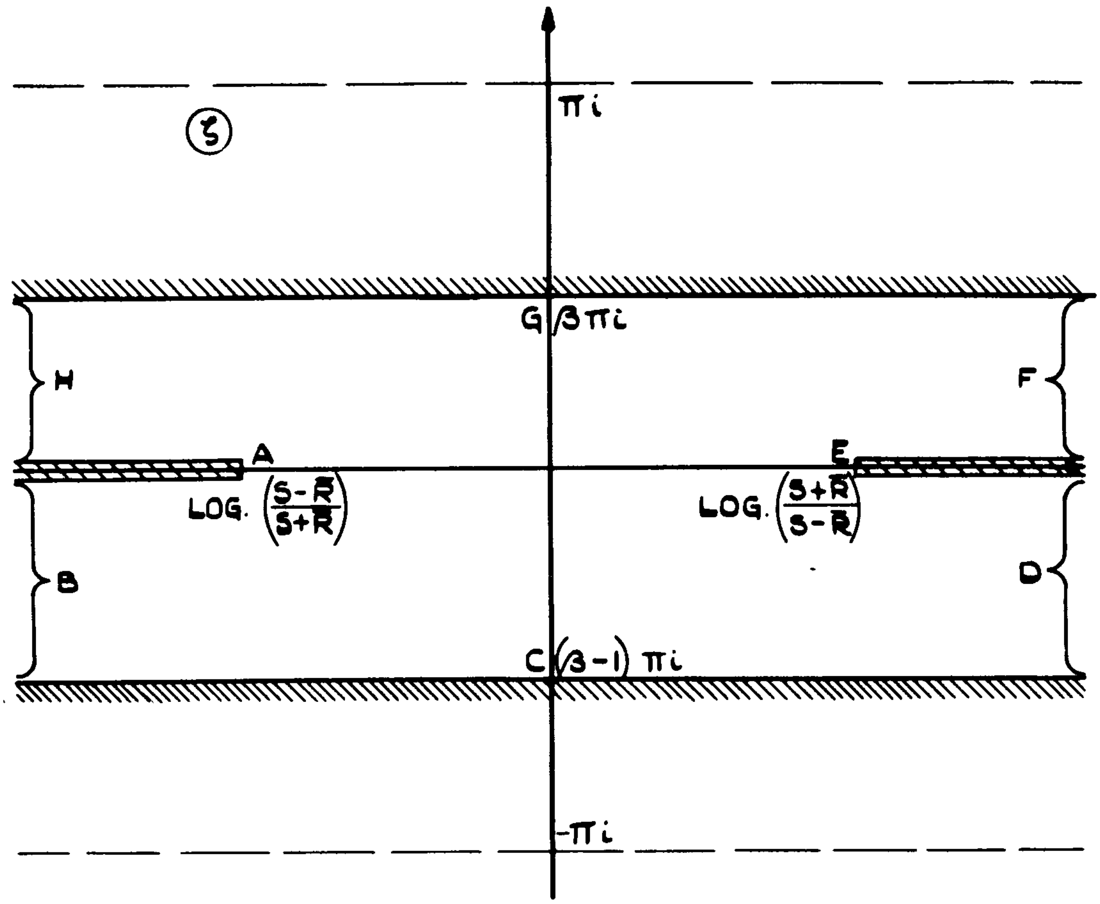

FIG. 2. FIRST TRANSFORMED PLANE - GENERAL CASE

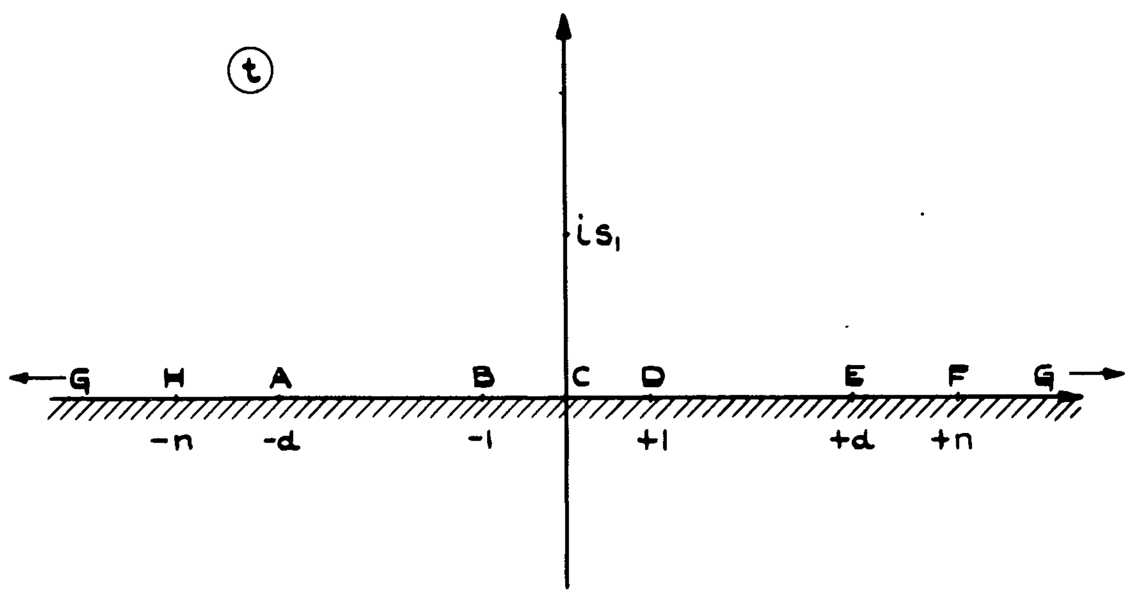

FIG.3 SECOND TRANSFORMED PLANE-GENERAL CASE

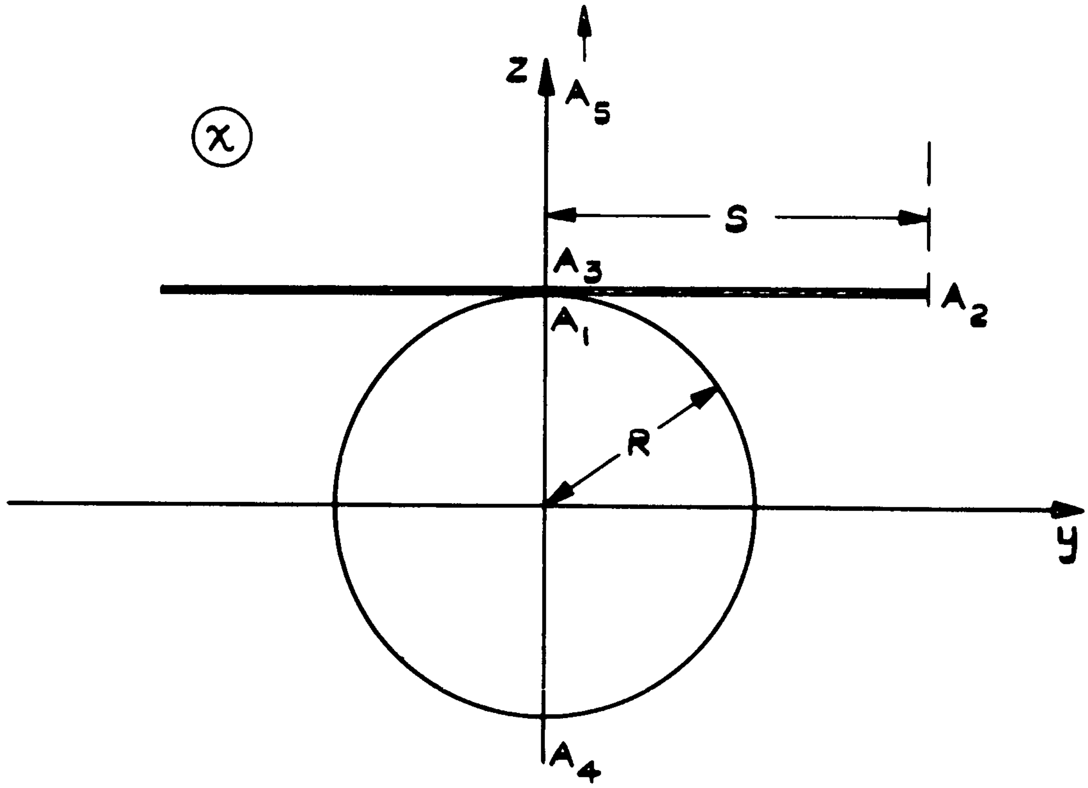

FIG. 4. SECTION OF THE CONFIGURATION BY A PLANE NORMAL TO FREE STREAM (CASE $\beta=0$)

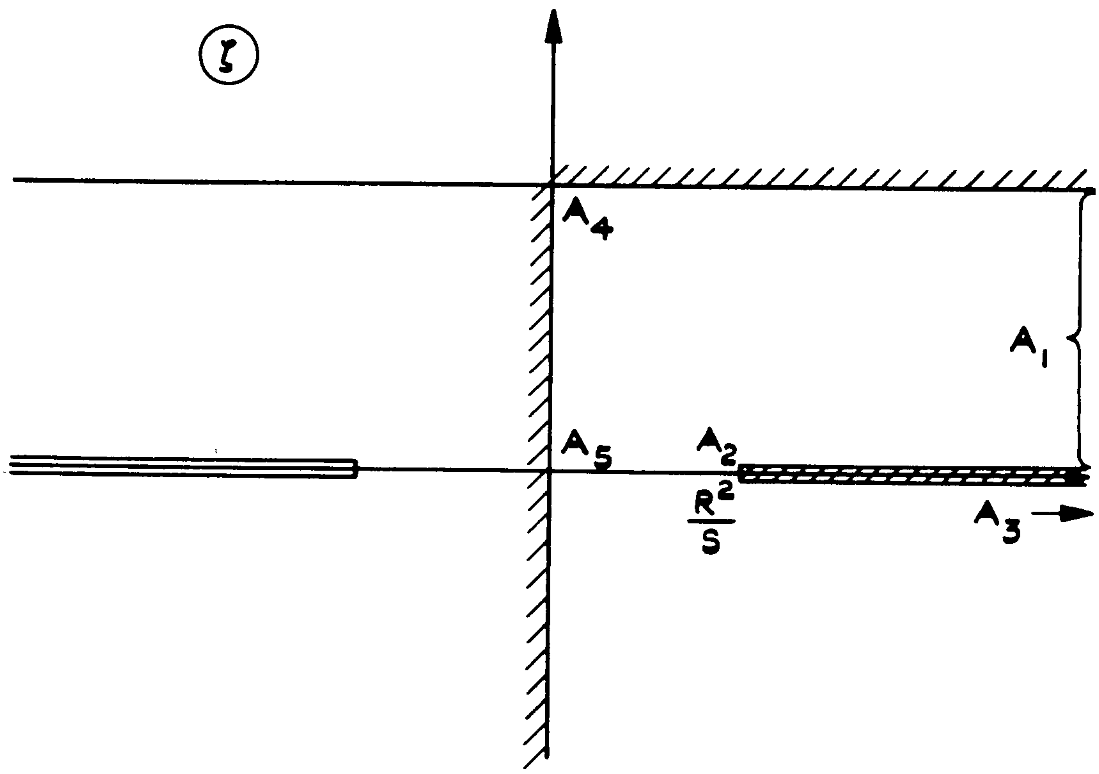

FIG. 5. FIRST TRANSFORMED PLANE (CASE $\beta=0$)

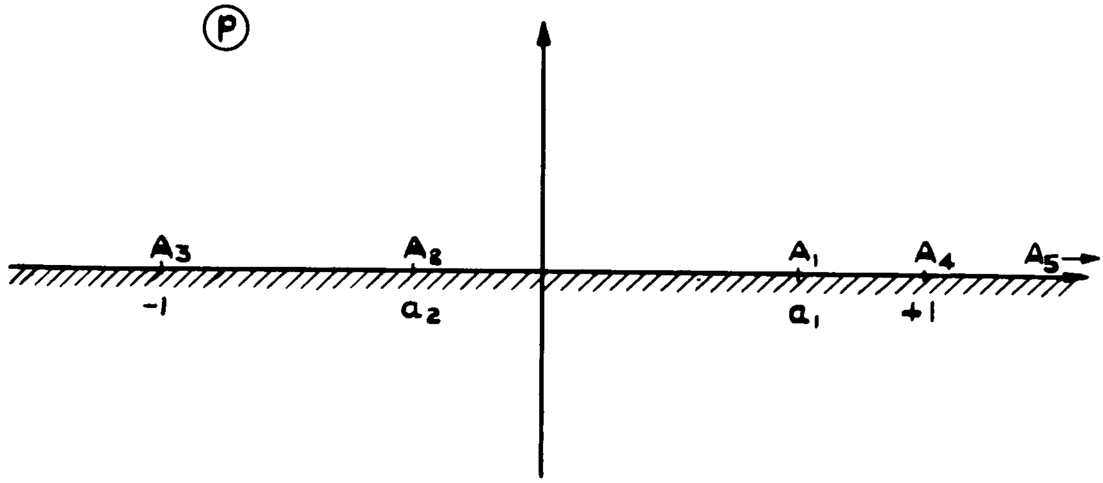

FIG. 6. THE SECOND TRANSFORMED PLANE (CASE $\beta = 0$)

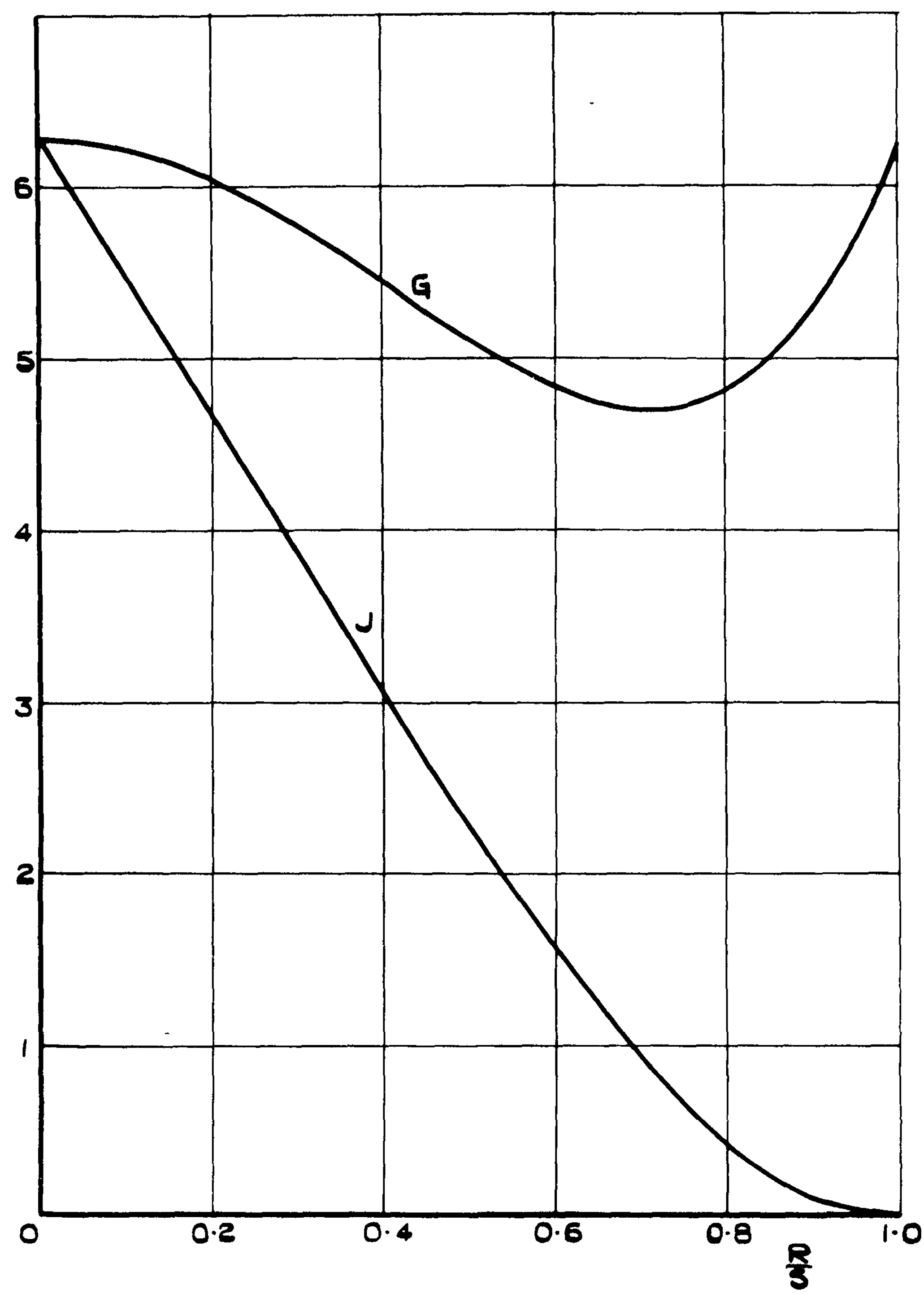

FIG. 7. $J\left(\frac{1}{2}, \frac{R}{S}\right)$ & $G\left(\frac{1}{2}, \frac{R}{S}\right)$

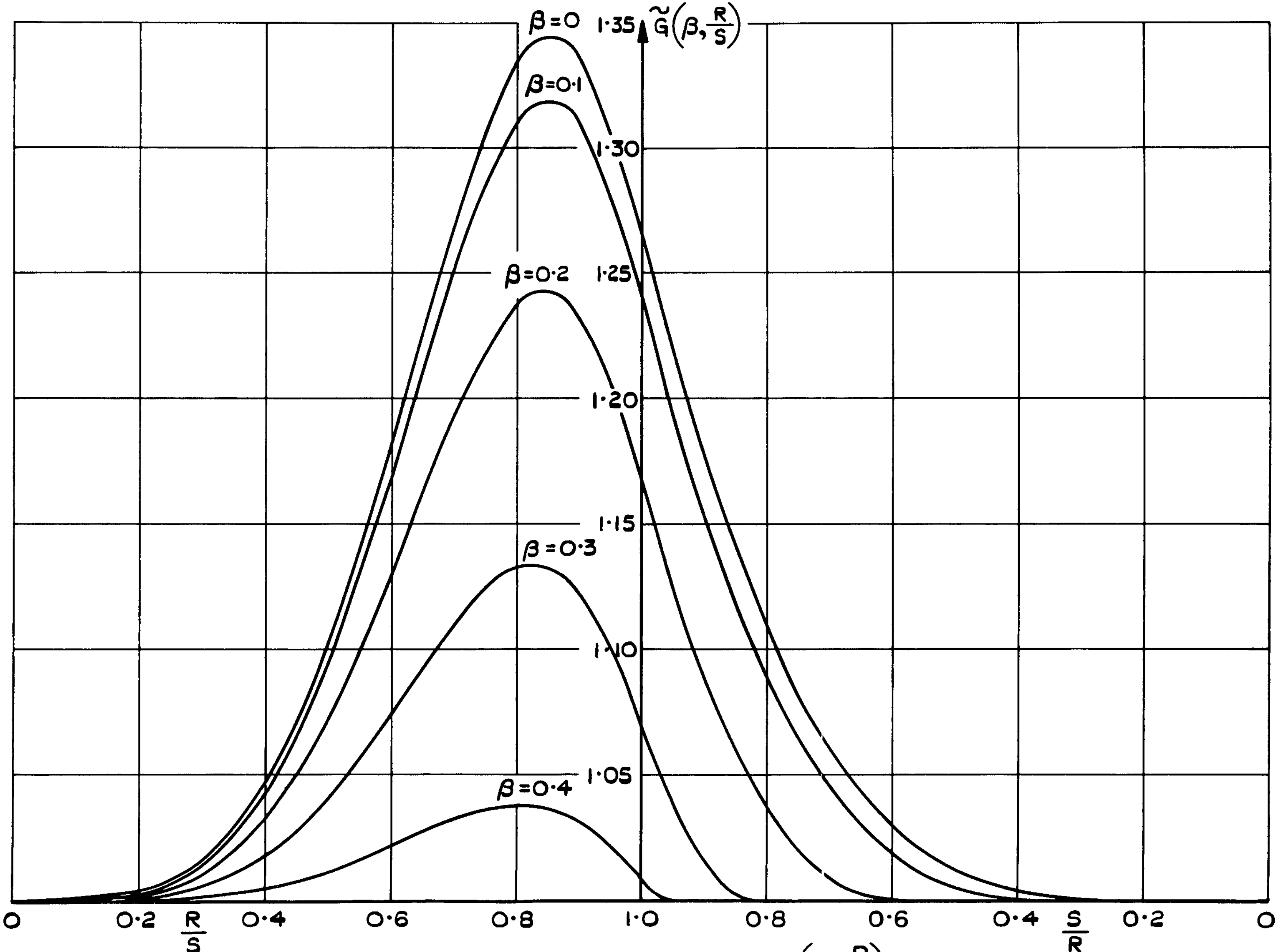

FIG. 8. THE FUNCTION $\tilde{G}\left(\beta, \frac{R}{S}\right)$

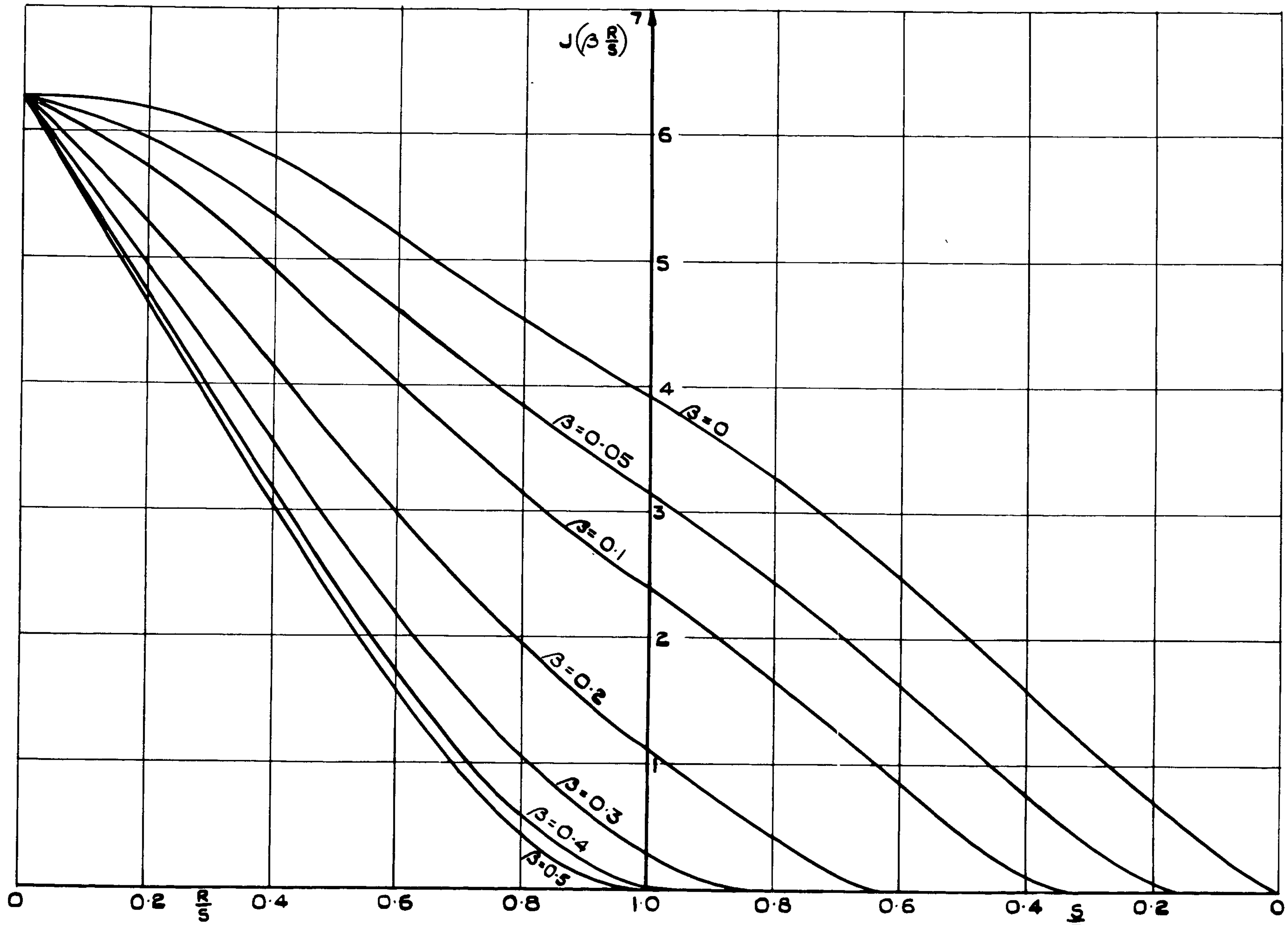

FIG. 9. THE FUNCTION $J\left(\beta, \frac{R}{S}\right)$, FOR VARIOUS VALUES OF β

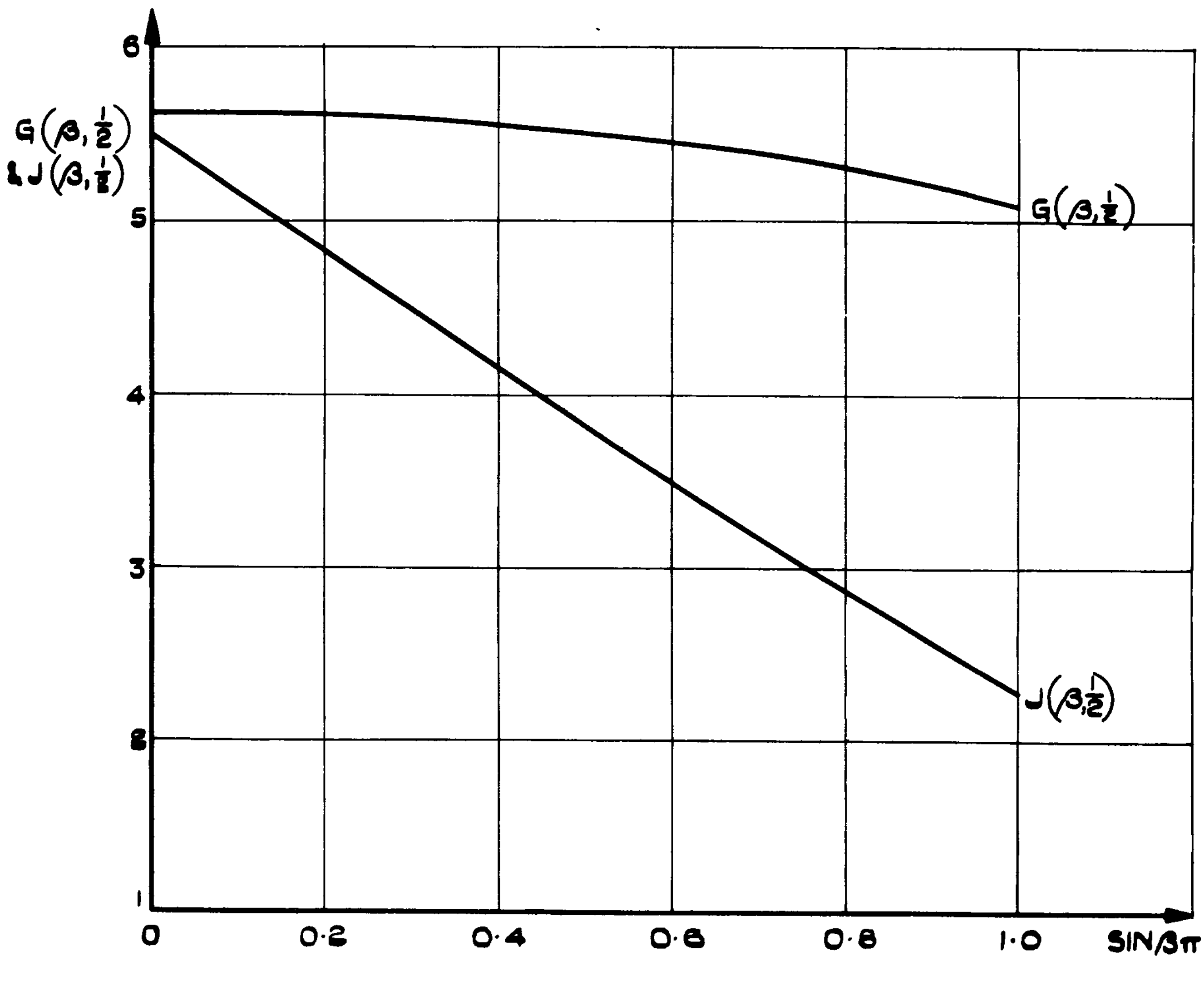

FIG.10. GRAPH SHOWING CHARACTERISTIC VARIATION OF $G\left(\beta,\frac{R}{S}\right)$ & $J\left(\beta,\frac{R}{S}\right)$ WITH SIN $\beta\pi$, FOR A TYPICAL VALUE OF $\frac{R}{S}$ (= 0·5)

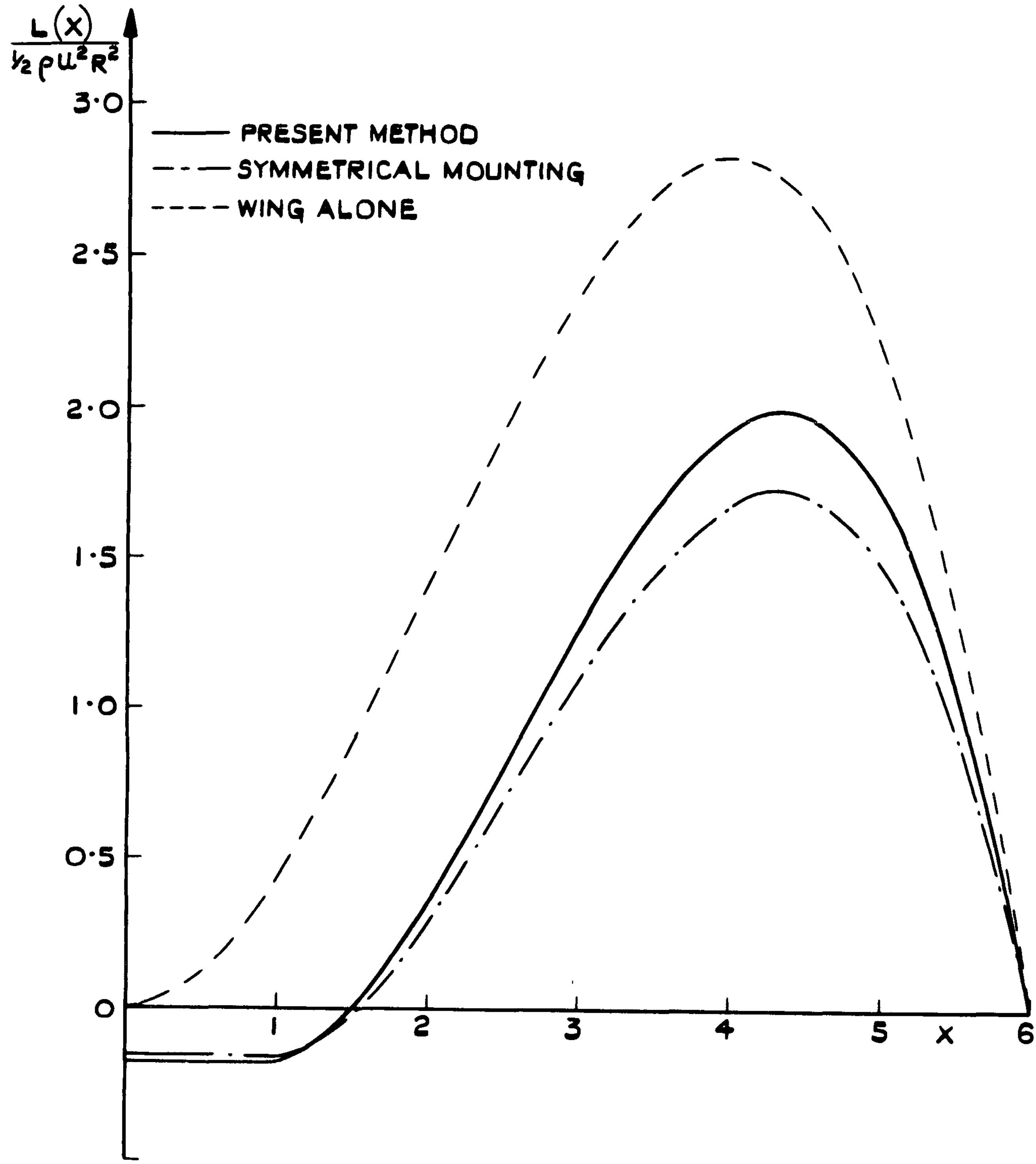

FIG. 11. CHORDWISE DISTRIBUTION OF LOCAL TOTAL LOAD FOR THREE CONFIGURATIONS EACH AT ZERO OVERALL LOAD.

Printed in England for Her Majesty's Stationery Office by the Royal Aircraft Establishment, Farnborough. W.T.61. K.4.

A.R.C. C.P. No.830

533.695.12 :
533.6.013.13 :
533.6.013.15

SLENDER-BODY THEORY CALCULATIONS OF THE EFFECT ON LIFT AND MOMENT OF MOUNTING THE WING OFF THE FUSELAGE CENTRE-LINE.
Bartlett, R.S. February 1964.

Slender-body theory is used to calculate the effects on lift and moment of mounting the wing of a wing-body combination above or below the body axis, with and without wing-body angle. The wing must have a local span which increases in the downstream direction, an unswept trailing edge and uncambered cross-sections. The cross-sections of the body are assumed to be circles of constant radius over the length of the wing.

It is found that the effects of the asymmetrical mounting are substantial when the body diameter is more than half the wing span, but fall off as the body shrinks. For a typical aircraft configuration, the pitching moment is found to be more affected than the lift.

A.R.C. C.P. No.830

533.695.12 :
533.6.013.13 :
533.6.013.15

SLENDER-BODY THEORY CALCULATIONS OF THE EFFECT ON LIFT AND MOMENT OF MOUNTING THE WING OFF THE FUSELAGE CENTRE-LINE.
Bartlett, R.S. February 1964.

Slender-body theory is used to calculate the effects on lift and moment of mounting the wing of a wing-body combination above or below the body axis, with and without wing-body angle. The wing must have a local span which increases in the downstream direction, an unswept trailing edge and uncambered cross-sections. The cross-sections of the body are assumed to be circles of constant radius over the length of the wing.

It is found that the effects of the asymmetrical mounting are substantial when the body diameter is more than half the wing span, but fall off as the body shrinks. For a typical aircraft configuration, the pitching moment is found to be more affected than the lift.

A.R.C. C.P. No.830

533.695.12 :
533.6.013.13 :
533.6.013.15

SLENDER-BODY THEORY CALCULATIONS OF THE EFFECT ON LIFT AND MOMENT OF MOUNTING THE WING OFF THE FUSELAGE CENTRE-LINE.
Bartlett, R.S. February 1964.

Slender-body theory is used to calculate the effects on lift and moment of mounting the wing of a wing-body combination above or below the body axis, with and without wing-body angle. The wing must have a local span which increases in the downstream direction, an unswept trailing edge and uncambered cross-sections. The cross-sections of the body are assumed to be circles of constant radius over the length of the wing.

It is found that the effects of the asymmetrical mounting are substantial when the body diameter is more than half the wing span, but fall off as the body shrinks. For a typical aircraft configuration, the pitching moment is found to be more affected than the lift.

C.P. No. 830

Published by
HER MAJESTY'S STATIONERY OFFICE

To be purchased from
York House, Kingsway, London w.c.2
423 Oxford Street, London w.1
13A Castle Street, Edinburgh 2
109 St. Mary Street, Cardiff
39 King Street, Manchester 2
50 Fairfax Street, Bristol 1
35 Smallbrook, Ringway, Birmingham 5
80 Chichester Street, Belfast 1
or through any bookseller

C.P. No. 830

S.O. CODE No. 23-9016-30